JOINT GLOBAL OCEAN FLUX STUDY

A Core Project of the International Geosphere-Biosphere Programme

JGOFS REPORT No. 36

PHOTOSYNTHESIS AND PRIMARY PRODUCTIVITY IN MARINE ECOSYSTEMS: PRACTICAL ASPECTS AND APPLICATION OF TECHNIQUES

July 2002

International Council for Science

Scientific Committee on Oceanic Research

Published in Bergen, Norway, July 2002 by:

Scientific Committee on Oceanic Research
Department of Earth and Planetary Sciences
The Johns Hopkins University
Baltimore, MD 21218
USA

and

JGOFS International Project Office
Centre for Studies of Environment and Resources
University of Bergen
5020 Bergen
NORWAY

The Joint Global Ocean Flux Study of the Scientific Committee on Oceanic Research (SCOR) is a Core Project of the International Geosphere-Biosphere Programme (IGBP). It is planned by a SCOR/IGBP Scientific Steering Committee. In addition to funds from the JGOFS sponsors, SCOR and IGBP, support is provided for international JGOFS planning and synthesis activities by several agencies and organizations. These are gratefully acknowledged and include the US National Science Foundation, the International Council of Scientific Unions (by funds from the United Nations Education, Scientific and Cultural Organization), the Intergovernmental Oceanographic Commission, the Research Council of Norway and the University of Bergen, Norway.

Citation: Photosynthesis and Primary Productivity in Marine Ecosystems: Practical Aspects and Application of Techniques. July 2002

ISSN: 1016-7331

Cover: JGOFS and SCOR Logos

The JGOFS Reports are distributed free of charge to scientists involved in global change research.

Additional copies of the JGOFS reports are available from:

Ms. Judith Stokke, Administrative Assistant
JGOFS International Project Office
Centre for Studies of Environment and Resources
University of Bergen
N-5020 Bergen, NORWAY

Tel: +47 5558 4246
Fax: +47 5558 9687
E-mail: *jgofs@uib.no*

or, from the International JGOFS website: *http://www.uib.no/jgofs/jgofs.html*

JOINT GLOBAL OCEAN FLUX STUDY

– JGOFS –

REPORT No. 36

PHOTOSYNTHESIS AND PRIMARY PRODUCTIVITY IN MARINE ECOSYSTEMS: PRACTICAL ASPECTS AND APPLICATION OF TECHNIQUES

TABLE OF CONTENTS

PHOTOSYNTHESIS AND PRIMARY PRODUCTIVITY

IN MARINE ECOSYSTEMS:

PRACTICAL ASPECTS AND APPLICATION OF TECHNIQUES

Edward Laws[1]

Egil Sakshaug[2]

Marcel Babin[3]

Yves Dandonneau[4]

Paul Falkowski[5]

Richard Geider[6]

Louis Legendre[7]

André Morel[8]

Morten Sondergaard[9]

Masayuki Takahashi[10]

Peter J. leB. Williams[11]

[1]University of Hawaii, Department of Oceanography, Honolulu, HI 96822-2285, USA

[2]Trondhjem Biological Station, Norwegian University of Science and Technology, Bynesvegen 46, N-7018 Trondheim, Norway

[3]University of California San Diego, Scripps Institution of Oceanography, 9500 Gilman Dr., La Jolla, CA 92093, USA

[4]LODYC, Université Pierre et Marie Curie, 4 Place Jussieu, F-75252 Paris cedex 05, France

[5]Rutgers University, Institute of Marine and Coastal Science, Environmental Biophysics and Molecular Ecology Program, 71 Dudley Road, New Brunswick, NJ, 08901-8521, USA

[6]Marine Biological Association of the United Kingdom, Citadel Hill, Plymouth PL1 2PB, United Kingdom

[7]Départment de Biologie, Université Laval, Québec, QC, G1K 7P4, Canada

[8]Laboratoire de Physique et Chimie Marines, B.P. 8, F-06230 Villefranche-sur-Mer, France

[9]Freshwater Biological Laboratory, University of Copenhagen, Helsingorsgade 51, Hillerod, DK-3400, Denmark

[10]Department of Biology, University of Tokyo, 3-8-1 Komaba, Meguro-ku, Tokyo 153, Japan

[11]School of Ocean Sciences, U.C.N.W, Menai Bridge, Gwynedd LL59 5EH, United Kingdom

ABSTRACT

The relationship between scalar irradiance (E_o) and photosynthetic rate per unit chlorophyll (P*) determined from short-term incubations with natural populations of phytoplankton in photosynthetrons or from measurements of the variable fluorescence yield of Photosystem II can be used to model photosynthetic rates in the ocean and, in conjunction with information derived from satellites, to estimate primary production on a basin or global scale. Care must be taken to accurately simulate both the intensity and spectral characteristics of submarine illumination to facilitate extrapolation of results obtained with artificial illumination to the water column. The analytical function and parameter values used to describe the relationship between the chlorophyll *a* normalized photosynthetic rate P* and scalar irradiance E_o are best determined using a least-squares procedure that weights observations relative to their contribution to the areal production integral. Such a least-squares procedures seeks to give the best possible description of $\frac{\mathrm{chl}\,P^*}{k\,E_o}$, where chl and k are the chlorophyll *a* concentration and visible light attenuation coefficient. The functional form of the P* vs. E_o relationship changes when instantaneous or short-term observations are replaced with photoperiod averages. In general, the photoperiod photosynthetic rate, $\overline{P}^*$, will be lower at a given average irradiance, $\overline{E}_o$, than the instantaneous or short-term rate P* at the same E_o. Analysis of field data indicates that mixed layer phytoplankton acclimate to irradiance in a way that maximizes P* at the average irradiance in the mixed layer. This condition is achieved when E_k ($=P_m^*/\alpha^*$) is 25-50% of the average irradiance. Under these conditions, calculated areal photosynthetic rates are more sensitive to P_m^*, the light-saturated photosynthetic rate, than to α^*, the initial slope of the P* vs. E_o curve.

INTRODUCTION

Phytoplankton biomass in the ocean amounts to about 1 petagram (Pg) of carbon[1], which is roughly 0.2% of the photosynthetically active carbon biomass on the Earth (Field et al., 1998). Nevertheless, the ocean is estimated to account for about 45-50% global net primary production (NPP), which is believed to be roughly 105 Pg of C y^{-1} (Field et al., 1998). The most recent estimates of oceanic NPP are based largely on data obtained from satellites (Platt and Sathyendranath, 1988; Sathyendranath et al., 1989; Morel and André, 1991; Lee et al., 1996; Behrenfeld and Falkowski, 1997a) and are almost two times greater than estimates made prior to the availability of ocean color data provided by satellites (Koblentz-Mishke et al., 1970; Woodwell et al., 1978). Although information on ocean color derived from satellites provides a comprehensive data set with which to estimate phytoplankton biomass, calculating marine primary productivity from remotely sensed information requires regional data on phytoplankton photosynthetic characteristics, which are still much undersampled (Longhurst et al., 1995). In order to achieve a global synthesis of carbon fluxes in the sea, mathematical models must be used, with light, temperature, nutrients, and chlorophyll *a* (chl *a*) concentrations as input variables. What is needed is not information on net carbon fixation at a few places, but a set of mathematical relationships between the above variables and the photosynthetic carbon flux, i.e., primarily the parameters of functions that relate phytoplankton carbon fixation rates to temperature, irradiance and chl *a* concentrations or light absorption.

The physiological responses of phytoplankton vary as a function of light regime, temperature, and nutritional status. A major goal in understanding how ocean dynamics affect phytoplankton production and carbon cycles is to determine how photosynthetic processes respond to geochemical and physical phenomena. Understanding these relationships is critical to developing prognostic models of the forcing and feedbacks between phytoplankton dynamics

[1] One petagram = 10^{15} grams = 1 gigatonne.

and ocean circulation. Even if there is presently a general understanding of photosynthetic responses to environmental variations, major difficulties remain regarding the application of this knowledge to specific oceanographic regimes. One strategy for developing reliable mathematical models to calculate photosynthetic rates under present-day ocean forcing, as well as under climatically altered forcing regimes, is to exploit theoretical constructs of photosynthetic responses and apply these constructs to empirical measurements. Such an approach rests on the assumption that the behavior of composite variables can be related to geochemical and physical processes more readily than the complex variables derived from purely empirical approaches.

This paper is the product of a Joint Global Ocean Flux Study (JGOFS) Photosynthesis Measurement Workshop held 17-21, August 1997 in Svalbard, Norway. It presents and discusses theoretical and practical considerations relevant to determining the relationship between irradiance and carbon uptake by phytoplankton as estimated by the ^{14}C method (Steemann-Nielsen, 1952) and to estimating light absorption by phytoplankton. The paper also deals at length with the physiological interpretation of parameters associated with photosynthesis-irradiance (P vs. E) curves. Finally, the paper discusses the relationship of core profiles and P vs. E curves to satellite maps of ocean color and estimates of basin scale primary production. It is complementary to the earlier report of Sakshaug et al. (1997) in the sense that it addresses practical aspects of implementing the theory presented in that publication.

DEFINITIONS AND THEORETICAL BACKGROUND

General

In oxygenic photosynthesis, the term "gross photosynthesis" is the light-dependent rate of electron flow from water to terminal electron acceptors such as CO_2 in the absence of any respiratory losses. It follows from this definition that gross photosynthesis is directly proportional to linear photosynthetic electron transport and hence, gross oxygen evolution (Falkowski and Raven, 1997, p. 264). Strictly speaking, gross photosynthesis should be defined on the basis of oxygen evolution rather than carbon fixation. The distinction is significant if photorespiratory rates are high or if a substantial fraction of photosynthetically generated electrons are used to reduce nitrate (Falkowski and Raven, 1997).

The respiration rate of photosynthetic organisms is the rate of electron flow from organic carbon to O_2 (or, in the case of anaerobic photosynthetic bacteria, to another electron acceptor) with the concomitant production of CO_2 (Falkowski and Raven, 1997). The difference between gross photosynthesis and the respiration of photosynthetic organisms during the photoperiod is net photosynthesis. When measured in terms of carbon, net photosynthesis includes organic carbon incorporated into biomass or excreted into the environment as dissolved organic carbon (Williams, 1993). In other words, net photosynthesis is the net amount of organic carbon produced by photoautotrophs in the light. The net rate of O_2 evolved per CO_2 fixed on a molar basis is called the photosynthetic quotient (PQ) and typically lies in the range 1.1-1.4 (Laws, 1991; Williams and Robertson, 1991). The value of the PQ reflects the relative amounts of the major macromolecules (polysaccharides, proteins, lipids, and nucleic acids) synthesized by the phytoplankton and the relative contribution of nitrate, ammonium, and urea as sources of nitrogen. High PQs reflect use of nitrate as a nitrogen source (Myers, 1980; Langdon, 1988; Laws, 1991; Williams and Robertson, 1991).

Gross primary production is the total amount of electron equivalents originating from the photochemical oxidation of water and is identical to gross photosynthesis (Falkowski and Raven, 1997, p. 264). Net primary production (NPP) refers to the organic carbon produced by photosynthetic processes within a specific period of time (e.g., day, year) that is subsequently made available to other trophic levels (Lindeman, 1942). NPP equals net photosynthesis minus photoautotrophic respiration that occurs during the dark period.

The terms primary productivity and primary production are frequently confused in the literature. Productivity is, strictly speaking, a time-dependent process with units of mass per unit time or mass per unit time per unit volume (or area). Production, while referenced to a (presumably) ecologically relevant period of time, is a quantity with units of mass or mass per unit volume (or area). For example, annual primary production in the ocean is currently estimated to be about 45-50 Pg of carbon (Field et al., 1998). Annual primary production at station ALOHA in the North Pacific subtropical gyre is about 170 g C m^{-2} (Letelier et al., 1996). However, primary productivity at station ALOHA varies from a low of 324 mg C m^{-2} d^{-1} in December to a high of 657 mg C m^{-2} d^{-1} in May (Fig. 1).

Irradiance

Because any absorbed photon with a wavelength in the range 350-700 nm is equally effective in producing a photochemical charge separation, it is convenient to express the amount of radiant energy that fuels photosynthesis in terms of photons. Photosynthetically available radiation (PAR) has been defined with respect to the 350-700 nm wavelength interval by SCOR/UNESCO Working Group 15 (Tyler, 1966). For reasons related to the technical difficulty of measuring light in the near-ultraviolet region, this interval was reduced to 400-700 nm.

Neglecting the near-UV (350-400 nm) domain usually does not entail a significant error, because the contribution of this radiation range to the total (350-700 nm) is small, roughly 5-7% for the radiation incident at the ocean surface. In the clearest oligotrophic ocean waters, however, in which the near-UV radiation may be more penetrating than light of wavelengths > 500 nm, the near-UV proportion increases with depth and may represent as much as 15% of PAR near the bottom of the euphotic zone.[2]

The radiometric quantity relevant to studies of photosynthesis is the flux of PAR. This quantity is calculated by integrating irradiance, $E(\lambda)$, from 400 to 700 nm and may be expressed as a flux of energy (e.g., watts m^{-2}) or of photons (e.g., mol photons m^{-2} s^{-1}). Irradiance so integrated is designated by the symbol E.[3] Because phytoplankton cells are believed to collect radiant energy equally well from all directions, the meaningful measure of irradiance is scalar irradiance, E_o, which is the flux of energy or photons incident from all directions onto a spherical collecting surface. The energy ε of a photon is related to its wavelength by the equation $\varepsilon = hc/\lambda$, where h is Planck's constant, c is the speed of light in vacuum, and λ is the wavelength. Because of this relationship, PAR measurements in terms of power cannot be transformed to photon fluxes unless the spectral distribution of the irradiance is known, and vice-versa.

In order to calculate the light actually absorbed by the phytoplankton, one must know the concentration of chl *a* in the water and the mean chl *a* specific absorption coefficient for the phytoplankton, $\overline{a_\phi^*}$, with typical units of m^2 (mg chl *a*)$^{-1}$. The superscript * here indicates that

[2] The base of the euphotic zone is here assumed to correspond to the depth at which PAR is reduced to 1% of its value at the surface, although some net photosynthesis may occur between the 0.1% and 1% light levels (e.g., Venrick et al., 1973).

[3] The symbol E is here used to distinguish integrated irradiance from radiant intensity, which is designated with the symbol I and has units of energy or quanta per unit solid angle.

the absorption coefficient has been normalized to chl *a*, and the subscript ϕ indicates that the absorption is due to phytoplankton cells. $\overline{a_\phi^*}$ may be calculated from the equation

$$\overline{a_\phi^*} = (E_{PAR})^{-1} \int_{400nm}^{700nm} a_\phi^*(\lambda) E_o(\lambda) d\lambda \quad (1)$$

where

$$E_{PAR} = \int_{400nm}^{700nm} E_o(\lambda) d\lambda \quad (2)$$

It should be obvious from this definition that $\overline{a_\phi^*}$ is dependent on the spectral composition of the submarine scalar irradiance field (Laws et al., 1990). The attenuation of scalar irradiance due to phytoplankton absorption is equal to the product of the chl *a* concentration and $\overline{a_\phi^*}$ and has dimensions (typically) of m^{-1}.

From a mechanistic standpoint it is useful to regard a_ϕ^* as the product of n, the number of photosynthetic units (PSUs) and the functional cross section (σ_{PSU}) of an individual PSU, i.e.,

$$a_\phi^*(\lambda) = n s_{PSU}(\lambda) \quad (3)$$

Typical units of n and σ_{PSU} are mol O_2 (mol chl *a*)$^{-1}$ and m^2 (mol O_2)$^{-1}$, respectively. The value of n is the inverse of the Emerson-Arnold number (Emerson and Arnold, 1932). Extensive laboratory and field studies have indicated that the Emerson-Arnold number is relatively constant and averages 2,000-2,200 mol chl *a* (mol O_2)$^{-1}$ (Falkowski and Kolber, 1993). According to the Emerson and Arnold (1932) definition, a PSU is the functional oxygen-producing entity (Gaffron and Wohl, 1936) and consists of a number of Photosystem I (PSI) and

Photosystem II (PSII) reaction centers to which antennae pigments transmit absorbed light energy. σ_{PSU} displays the same spectral dependence as a_{ϕ}^{*}.

PHOTOSYNTHESIS-IRRADIANCE CURVES

Photosynthetic rates normalized to chl *a* concentrations are here designated P^{*} (Sakshaug et al., 1997). They are related to irradiance in a nonlinear manner. In order to quantify this relationship, P* vs. E_o data are needed. In a typical P* vs. E_o determination, a series of subsamples drawn from a single seawater sample with a known chl *a* concentration is incubated in a gradient of artificial light at a temperature as close as possible to natural conditions. Ideally the P* vs. E_o response should provide information on the physiological condition of the phytoplankton at the moment of sampling. Hence, the incubation time should be as short as possible. The mathematical description of the P* vs. E_o curve is incorporated into a bio-optical model, which allows areal production to be estimated from information on (typically) pigment profiles, temperature, and irradiance (Platt and Sathyendranath, 1993; Behrenfeld and Falkowski, 1997b).

Typical P* vs. E_o curve can be characterized by three major regions:

1 At the lowest irradiances, P* is almost directly proportional to E_o, i.e., the rate-limiting step in the photosynthetic process is the absorption of light

2 As E_o increases, the slope of the P* vs. E_o curve decreases, and P* eventually reaches a saturation level. At the saturation level, the rate of light absorption greatly exceeds the rate of steady-state electron transport from water to CO_2.

3 With further increase in irradiance, a reduction in P* relative to the saturation level may occur. This phenomenon, called photoinhibition, is dependent on both the irradiance and the duration of exposure.

Commonly used models of the relationship between irradiance and photosynthetic rate take one of the following forms (Jassby and Platt, 1976; Platt et al., 1980):

Rectangular hyperbola $$P^* = \frac{P_m^* E_o}{E_o + P_m^* / \alpha^*} \quad (4)$$

Negative exponential $$P^* = P_m^* (1 - e^{-E_o \alpha^* / P_m^*}) \quad (5)$$

Negative exponential with photoinhibition $$P^* = P_m^* (1 - e^{-E_o \alpha^* / P_m^*}) e^{-bE_o \alpha^* / P_m^*} \quad (6)$$

Hyperbolic tangent: $$P^* = P_m^* \tanh(E_o \alpha^* / P_m^*) \quad (7)$$

Piecewise linear: $$\begin{aligned} P^* &= \alpha^* E_o \quad E_o \le P_m^* / \alpha^* \\ &= P_m^* \quad E_o \ge P_m^* / \alpha^* \end{aligned} \quad (8)$$

In these equations, α^* is the initial slope of the P* vs. E_o curve, P_m^* is the light-saturated photosynthetic rate per unit chl *a* in the absence of photoinhibition, and b is a dimensionless photoinhibition parameter. The behavior of these five models is shown in Fig. 2. The ratio P_m^* / α^* has dimensions of irradiance and is denoted by the symbol E_k. In the absence of light inhibition, it is the irradiance at the intersection of the two tangents to the P* vs. E_o curve in the limit as $E_o \to 0$ and $E_o \to \infty$. In the photoinhibited model (Eq. 6), the maximum photosynthetic rate occurs when $E_o/E_k = \ln[(1 + b)/b]$ and equals P_m^* multiplied by $b^b/[(1 + b)^{(1 + b)}]$. Field data summarized by Platt et al. (1980) indicate that b averages about 0.03 (range: 0 – 0.06). Taking 0.03 as a working average for b implies that the maximum photosynthetic rate in the light-

inhibited model is about 87% of P_m^* (Fig. 2). At $E_o = E_k$, the ratio P^*/P_m^* equals 0.50, 0.63, 0.61, 0.76, and 1.0 for models 4-8, respectively. Although there are clearly systematic differences in the way these five functions describe the P* vs. E_o relationship, all five functions follow the general form $P^* = P_m^* f(\alpha^* E_o / P_m^*)$, where f is some function that equals zero at $E_o = 0$ and, with the exception of equation 3, equals 1 as $E_o \rightarrow \infty$. This fact is obvious in the case of models 5-7. In the case of the rectangular hyperbola, $f = 1/[P_m^*/(E_o\alpha^*) + 1]$. In the case of the piecewise linear function, $f = \alpha^* E_o / P_m^*$ for $E_o \leq P_m^*/\alpha^*$ and $f = 1$ for $E_o \geq P_m^*/\alpha^*$.

From a mechanistic standpoint, P_m^* may be regarded as the quotient of the number of photosynthetic units and their minimum turnover time, τ, i.e.,

$$P_m^* = n/\tau \tag{9}$$

P_m^* is independent of the spectral composition of the irradiance and is commonly referred to as an assimilation number. The maximum quantum yield ϕ_m is defined by the equation

$$\phi_m = \alpha^* / \alpha_\phi^* \tag{10}$$

and is usually reported in units of moles of carbon fixed or moles of O_2 produced per mol quanta absorbed. Strictly speaking, ϕ_m is spectrally dependent, because not all antennae pigments transmit absorbed light to photosynthetic reaction centers with equal efficiency. Furthermore, photoprotective pigments such as β-carotene and zeaxanthin do not transfer excitation energy to reaction centers at all, but instead screen the cell from excess light (Falkowski and Raven, 1997). In practice, however, ϕ_m is usually treated as a spectrally independent parameter, causing it to

become variable (Sakshaug et al., 1997). ϕ_m may be regarded as the ratio of the functional absorption cross section of PSII (σ_{PSII}) to σ_{PSU}, i.e.,

$$\phi_m = \sigma_{PSII} / \sigma_{PSU} \quad (11)$$

where σ_{PSII} has typical units of m^2 (mol quanta)$^{-1}$ and, like σ_{PSU}, is spectrally dependent. Combining equations 3, 10, and 11 gives

$$\alpha^* = \phi_m n \sigma_{PSU} = n \sigma_{PSII} \quad (12)$$

SOURCES OF VARIABILITY IN PHOTOSYNTHETIC PARAMETERS

Assuming the average size of a PSU to be 2000 chlorophyll/O_2 and the associated turnover time to be 1.0 millisecond, Falkowski (1981) estimated an upper bound on P_m^* to be 2.0 moles O_2 (gram chl *a*)$^{-1}$ h^{-1}. Assuming a PQ of 1.1-1.4, this estimate translates into 17- 22 g C (g chl *a*)$^{-1}$ h^{-1}. As noted by Falkowski (1981), such high assimilation numbers are rarely reported and require that photosynthesis be limited by neither nutrients nor temperature. More commonly reported assimilation numbers generally lie in the range 2-10 g C (g chl *a*)$^{-1}$ h^{-1} (Harrison and Platt, 1980; Platt et al., 1982; Vedernikov, 1982; Laws et al., 1987; Sathyendranath et al., 1996, 1999; Renk and Ochocki, 1998; Gaxiola-Castro et al., 1999; Renk et al., 1999), although values as low as 0.1 or less have been reported for sea ice microalgae (Palmisano and SooHoo, 1985). The lower values presumably reflect slower PSU turnover times and/or larger photosynthetic units (see below).

Based on the Z scheme of photosynthesis, eight photons are required to produce one molecule of O_2 (Kok, 1948). Hence an upper bond on ϕ_m should be about 0.125 mole O_2 per mole quanta, and values of ϕ_m reported for laboratory cultures of phytoplankton may indeed be

as high as 0.10-0.12 mole O_2 per mole quanta (Myers, 1980; Ley and Mauzerall, 1982). When expressed in units of moles C fixed per mole quanta, ϕ_m is typically as low as 0.06-0.08. This difference reflects in part the fact that the PQ typically lies in the range 1.1-1.4 moles O_2 per mole C. In natural communities, however, values of ϕ_m based on measurements of α^* and $\overline{a_\phi^*}$ or derived from measurements of variable fluorescence are highly variable and can be less than 0.005 in oligotrophic areas. Oligotrophy in combination with strong light may cause particularly low values (Lewis et al., 1988; Cleveland et al., 1989; Bidigare et al., 1990b; Schofield et al., 1993; Babin et al. 1996).

Causes of variability in ϕ_m and P* vs. E_o parameters include the following:

1 Absorption of light by pigments that do not transfer the absorbed energy to the photosynthetic reaction centers decreases α^* and hence ϕ_m and E_k. These photoprotective pigments are often most evident at high irradiances during nutrient deprivation.

2 Loss of functional reaction centers reduces n and hence lowers α^* and P_m^*. According to studies of the quantum yield of fluorescence of phytoplankton cultures, n is a maximum when cells are nutrient-replete. These studies also indicate that n may be remarkably independent of species and low in nutrient-deprived cells (Kolber et al., 1988; Falkowski. 1992; Vassiliev et al., 1995). In the upper portion of the nutrient-impoverished subtropical gyres and in the nutricline (100-125 m), n may be reduced by 40-70% and 25%, respectively (Falkowski and Kolber, 1995).

3 Cyclic electron flow decreases σ_{PSII} and increases σ_{PSU}. Hence cyclic electron flow lowers both α^* and ϕ_m and increases E_k. In cyanobacteria, cyclic electron flow around PSI generates ATP and is essential to support metabolism, especially nitrogen fixation. Such a

cycle uses photons but does not lead to a reduction of CO_2 and hence causes the quantum yield to decline. At high irradiances, electrons can cycle around PSII, bypassing the oxidation of the water-splitting complex (Prasil et al., 1996). This cycle is protective, because it dissipates excess excitation.

4 Photorespiration is a consequence of the fact that the principal carbon-fixing enzyme, Ribulose-1,5-bisphosphate carboxylase/oxygenase (Rubisco), can accept O_2 as a substrate. The products of this reaction are phosphoglycolate and 3-phosphoglycerate. The latter product enters the usual photosynthetic pathway. Reduction of one 3-phosphoglycerate molecule to glyceraldehyde-3-phosphate requires one NADPH and produces half an oxygen molecule. The former product, phosphoglycolate, is hydrolyzed to produce phosphate and glycolate. Some of the glycolate is excreted, but the majority is further metabolized. Metabolism of the glycolate releases 0.25-1.0 mole of CO_2 per mole of glycolate carbon, leaving 0-0.75 mole of carbon available for biosynthesis (Raven, 1984a,b; 1993). Since the oxidation of one molecule of glycolate consumes one molecule of O_2 and releases two molecules of CO_2, the photosynthetic quotient in the presence of photorespiration becomes $(PQ - 0.5x - \gamma x)/(1 - 2\gamma x)$, where PQ is the photosynthetic quotient in the absence of photorespiration, x is the ratio of oxygenase to carboxylase activity, and γ is the fraction of glycolate carbon that is completely oxidized to CO_2. This ratio is independent of x if $\gamma = 0.5/(2PQ - 1)$. If γ is greater than $0.5/(2PQ - 1)$, photorespiration will lead to an increase in the photosynthetic quotient. If γ is less than $0.5/(2PQ - 1)$, photorespiration will cause the photosynthetic quotient to decrease. For typical PQs (1.1 – 1.4), the critical range of γ is 0.28 – 0.42. In general, then, it is impossible to say whether photorespiration will cause an increase or decrease in the

photosynthetic quotient, but photorespiration will certainly decrease the rate of O_2 production and CO_2 uptake. The result will be a decrease in α^* and P_m^*. In terrestrial C_3-plants photorespiratory consumption of O_2 can account for 25% of Rubisco activity (Falkowski and Raven, 1997). In marine phytoplankton the existence of a CO_2-concentrating mechanism appears to be quite common (Raven and Beardall, 1981; Weger et al., 1989), and for this reason photorespiration is assumed to be of minor importance in marine phytoplankton compared to terrestrial C_3 plants (Laws et al., 2000).

5 The packaging of pigments within the cell reduces $\overline{a_\phi^*}$ and σ_{PSII}. This causes α^* and E_k to decrease and increase, respectively. The packaging effect is physical in the sense that pigments packed into chloroplasts are less efficient in absorbing light per unit pigment mass than pigments dispersed in an optically thin medium (Duysens, 1956; Geider and Osborne, 1987; Berner et al., 1989; Sakshaug et al., 1997). The packaging effect depends on both the cell size and pigment concentration/ratios in the cell (Kirk, 1975; Morel and Bricaud, 1981). The effect is wavelength-dependent and is most pronounced where absorption is greatest. The packaging effect is generally more pronounced in large and pigment-rich (i.e., shade-acclimated) cells.

Estimation of Photosynthetically Usable Radiation (PUR)

Phytoplankton do not absorb all wavelengths of light with equal efficiency, and bio-optical modelers have developed the concept of photosynthetically useable radiation (PUR) to reflect this inefficiency (Morel, 1978). Photosynthetically useable irradiance (E_{PUR}) is defined by the equation

$$E_{PUR} = E_{PAR}\left(\overline{a_{\phi}^{*}} / a_{\phi\,m}^{*}\right) \quad (13)$$

where $\overline{a_{\phi}^{*}}$ is the mean chl *a*-specific absorption coefficient for the phytoplankton (Eq. 1) and $a_{\phi\,m}^{*}$ is the maximum value of $a_{\phi}^{*}(\lambda)$, which typically occurs at a wavelength of ~440 nm. The spectral characteristics of the artificial light in a photosynthetron (Lewis and Smith, 1983; Lohrenz et al., 1992; Morel et al., 1996) or similar incubator virtually never duplicate those of the submarine irradiance field at the depth from which a sample of seawater was collected. This point is moot if the irradiance in the incubator is spectrally resolved (Lewis et al., 1985a,b), but when this is not the case, calculation of P* vs. E_o curves using E_{PUR} as the independent variable rather than E_{PAR} is a convenient way to correct for the spectral differences between artificial light and natural submarine irradiance (e.g., Morel et al., 1996). In effect, calculations are based on absorbed light rather than incident light, with $a_{\phi\,m}^{*}$ being a convenient normalization factor. The problem with basing calculations on absorbed light is the fact that antennae pigments do not all transmit absorbed light to photosynthetic reaction centers with equal efficiency, i.e., the quantum yield has a spectral dependence. Furthermore, as noted, photoprotective pigments do not transfer excitation energy to reaction centers at all.

Given their ecological role, photoprotective pigments not surprisingly contribute most to light absorption when $E_o >> E_k$ (e.g., Higgins and Mackey, 2000), and under these conditions modeled photosynthetic rates are much more sensitive to P_m^*, which is spectrally invariant, than to α^*, which is spectrally dependent (see below). Modeled photosynthetic rates are more sensitive to α^* than to P_m^* when $E_o < E_k$ (see below), and under these conditions a poor match between the spectral characteristics of the artificial light source in a photosynthetron and

submarine irradiance can lead to significant errors in the estimation of α^* due to the spectral dependence of the quantum yield.

Irradiance in incubator

No matter how much care is taken in the collection and manipulation of seawater samples, estimation of photosynthetic parameters will be compromised if the irradiances inside the incubators are not properly measured. Irradiance meters are best suited for measurements in a homogeneous light field. However, the complex geometry of the light source, the cooling system, the reflective walls of the incubators, and the irradiance meter itself make it difficult to accurately measure the effective irradiance during an incubation. In a photosynthetron the surfaces through which light penetrates or is reflected are likely to cause an inhomogeneous irradiance field. This problem can be overcome to some extent with the use of a 4π irradiance sensor small enough to be placed inside a vial. The sensor should be placed as close as possible to the center of the vial in a position that can be reproduced for all the vials in the photosynthetron. Since commercially available 4π sensors are often larger than the mouth of scintillation vials, it may be necessary to cut off the narrow mouth of a vial and to use this modified vial for irradiance measurements. In the radial photosynthetron described by Babin et al. (1994) incubations are carried out in 50-ml culture flasks whose mouths are typically wide enough to accommodate most 4π sensors. However, care must again be taken to obtain accurate measurements inside the flasks.

An alternative to the direct measurement of irradiance with a light meter is the use of a chemical actinometer. The original studies of chemical actinometers utilized uranyl oxalate (Leighton and Forbes, 1930), but this was later superseded by the use of an acidified solution of

potassium ferrioxalate (Hatchard and Parker, 1956; Seliger and McElroy, 1965; Welschmeyer and Lorenzen, 1981; Babin et al, 1994; Stramski et al., 1995). The procedure is straightforward. A dilute, non-quenching solution of ferric iron is placed in the incubation flasks and incubated for a short time, after which one measures the concentration of ferrous iron that has formed as a result of the exposure to the light. This chemical method circumvents the geometry problems associated with physical measurements, because the photoreactive molecules are distributed inside the incubation flasks in the same manner as the phytoplankton cells. The requirements of the actinometric method are constant quantum efficiency and a high absorption factor over a wide range of wavelengths and total radiation doses, and high sensitivity and precision. The ferrioxalate actinometer described by Hatchard and Parker (1956) satisfies most of these criteria, and its quantum yield is approximately 1.0 at wavelengths between 400 and 500 nm. However, the quantum yield drops dramatically at wavelengths greater than roughly 500 nm and rises to 1.1-1.2 in the wavelength range 350-400 nm (Hatchard and Parker, 1956). Because of the spectral dependence of the quantum yield, the actinometric method cannot be recommended for general photosynthetic work.

Irradiance in the water column

Accurate determination of the irradiance field in the water column is by no means trivial. Since only downwelling irradiance, E_d, penetrates the surface, irradiance measurements made above the surface require the use of an instrument equipped with a flat (cosine) collector. Use of an instrument equipped with a 4π sensor will overestimate the penetrating radiant flux. The magnitude of this overestimate can be as much as a factor of 2 for a zenith sun angle of 60° and a dark blue sky (Sakshaug et al., 1997). In the water column measurements should be made of

scalar irradiance using an instrument equipped with a 4π sensor. Both $E_o(\lambda)$ and E_{PAR} should be measured and recorded as a function of depth. Because of fluctuations originating from wave-induced lens effects and from variations in immersion depths, irradiance measurements made just below the surface are unreliable and their extrapolation toward the null depth very uncertain. The commonly adopted solution to this problem consists of measuring the incident downwelling irradiance in the air and correcting the measured value for reflective loss. This loss amounts to no more than 2-5% for zenith angles less than 45° but may exceed 10% of incident irradiance for low solar elevations, depending somewhat on the sea state and the contribution of sun versus sky irradiance (Jerlov, 1968; Morel and Antoine, 1994). Substitution of E_d (corrected for reflection) for the scalar irradiance just below the surface obviously assumes that upwelling irradiance is negligible at the surface.

If penetration of light into the sea cannot be measured, it may instead be predicted from information on incident E_{PAR} recorded above the surface and from the vertical distribution of chl *a*, at least in Case I waters (Baker and Smith, 1982; Morel, 1988). The prediction in Case II waters is more complicated and requires additional information (often unavailable) on other optically active constituents.

Spectral characteristics

A number of investigators have explored the implications of failure to mimic the spectral characteristics of submarine light in simulated in situ incubations. Kiefer and Strickland (1970) incubated natural populations from California coastal waters under both white light and blue light, the latter having spectral characteristics similar to Case II ocean water. They reported that photosynthetic rates were about 66% higher under blue light if the neutral density filters were

chosen so as to equalize the energy fluxes in each pair of blue and white light incubators. Morel et al. (1987) examined the photosynthetic characteristics of the diatom *Chaetoceros protuberans* to changes in light intensity and color. They found that the initial slope of the P* vs. E_o curve was about 81% higher when the cells were grown in blue light versus white or green light. If their results were recalculated in terms of absorbed radiation rather than incident radiation, the initial slopes were identical, independent of color. In other words, the differences were due to the degree of match/mismatch between the spectrum of the light and the light absorption spectrum of the diatom. Laws et al. (1990) measured the photosynthetic rates and pigment composition of phytoplankton communities in the North Pacific subtropical gyre. They found that the chl *a* specific absorption coefficient of the phytoplankton was almost 3 times greater in blue light than in white light and concluded that areal primary production rates could be underestimated by about a factor of 2 in the open ocean if incubations were conducted using surface light attenuated with neutral density filters.

When α^* is calculated with respect to E_{PUR}, one source of error is the estimation of $\overline{a_\phi^*}$ in equation 13. To appreciate the effect of errors in $a_\phi^*(\lambda)$ and $E_o(\lambda)$ on $\overline{a_\phi^*}$, we rewrite the integral on the right-hand side of equation 1 in the form

$$\begin{aligned}\int_{400nm}^{700nm} a_\phi^*(\lambda)E_o(\lambda)d\lambda \;=\; &\int_{400nm}^{700nm} a_{\phi e}^*(\lambda)E_{oe}(\lambda)d\lambda \\ &+ \int_{400nm}^{700nm} \Delta a_\phi^*(\lambda)E_o(\lambda)d\lambda \;+ \int_{400nm}^{700nm} a_\phi^*(\lambda)\Delta E_o(\lambda)d\lambda \\ &- \int_{400nm}^{700nm} \Delta a_\phi^*(\lambda)\Delta E_o(\lambda)d\lambda\end{aligned} \qquad (14)$$

where $a^*_{\phi e}(\lambda)$ and $E_{oe}(\lambda)$ are the estimated chl *a* specific absorption coefficient and irradiance at wavelength λ, respectively, $\Delta a^*_\phi(\lambda) = a^*_\phi(\lambda) - a^*_{\phi e}(\lambda)$ and $\Delta E_o(\lambda) = E_o(\lambda) - E_{oe}(\lambda)$. Ideally the error terms $\Delta a^*_\phi(\lambda)$ and $\Delta E_o(\lambda)$ have an expectation value of zero and are uncorrelated with $E_o(\lambda)$ and $a^*_\phi(\lambda)$, respectively, and with each other, in which case, the expectation value of the left-hand side of equation 14 equals the expectation value of $\int_{400nm}^{700nm} a^*_{\phi e}(\lambda) E_{oe}(\lambda) d\lambda$. In other words, the expectation value of $\overline{a^*_{\phi e}}$ is $\overline{a^*_\phi}$. Assuming that the errors in $a^*_\phi(\lambda)$ and $E_o(\lambda)$ are small, most of the error in $\overline{a^*_{\phi e}}$ will come from the second and third integrals on the right-hand side of equation 14. If submarine irradiance is assumed to have the same spectral characteristics as surface light, for example, $\Delta E_o(\lambda)$ will be positive in the blue region of the spectrum and negative at longer wavelengths. Since $a^*_\phi(\lambda)$ is greatest toward the blue end of the spectrum, the expectation value of $\int_{400nm}^{700nm} a^*_\phi(\lambda) \Delta E_o(\lambda) d\lambda$ will be positive, and the expectation value of $\overline{a^*_{\phi e}}$ will be less than $\overline{a^*_\phi}$. As noted above, this error can cause as much as a factor of 3 underestimation of $\overline{a^*_\phi}$.

Another potential source of systematic bias is the contribution of detrital and other non-algal absorption to $\overline{a^*_{\phi e}}$. Detritus is expected to increase absorption in the blue and to produce a spectrum with, “little spectral structure, exhibiting a steep decrease in relative absorption going from the blue to the red” (Mitchell and Kiefer, 1988, p. 683). To the extent that non-algal

particles contribute to light absorption, the integral $\int_{400nm}^{700nm} \Delta a_{\phi}^{*}(\lambda) E_o(\lambda) d\lambda$ will be negative, and this fact will cause $\overline{a_{\phi e}^{*}}$ to overestimate $\overline{a_{\phi}^{*}}$. The extent of the overestimation will be greatest when the submarine irradiance field is dominated by blue light.

Naively one might assume that $a_{\phi}^{*}(\lambda)$ could be reconstructed by extracting algal pigments, measuring their concentrations, and summing the product of their concentrations and specific absorption coefficients at each wavelength. Several factors potentially confound such reconstructions. First, the *in vivo* absorption spectra of the pigments are shifted by about 10 nm toward longer wavelengths (Bricaud et al., 1983). Second, packaging effects reduce *in vivo* absorption, particularly in the blue region of the spectrum (Laws et al., 1990; Johnsen and Sakshaug, 1993). In practice, however, it is often straightforward to correct for spectral shifts and package effects (Hoepffner and Sathyendranath, 1991), and in many cases package effects appear to be minimal. Nelson et al. (1993), for example, found that measurable package effects occurred in less than 25% of samples collected over a 250-km transect across a highly variable region of the Southern California Bight. In cases where reconstructed phytoplankton absorption spectra overestimated measured spectra, most of the differences could be reconciled by application of an algorithm that corrected for packaging effects.

A widely used alternative to reconstructing absorption spectra from extracted pigments is to concentrate particles on a glass-fiber filter and measure their absorption spectrum with a filter blank as a reference (Trüper and Yentsch, 1967). The procedure requires using a spectrophotometer equipped with an integrating sphere or another optical arrangement for the collection of light scattered by particles. Unfortunately, the absorption spectrum obtained using this simple and rapid technique is strongly affected by pathlength amplification induced by

multiple scattering within the filter and between the filter and particles. The pathlength amplification factor varies with optical density and hence with wavelength and filter type (Mitchell, 1990; Cleveland and Weidemann, 1993). Species-independent algorithms have been proposed to correct for pathlength amplification, but these algorithms may lead to serious errors for some phytoplankton groups (Moore et al., 1995).

A third approach that overcomes the pathlength amplification problem is a modification of the filter-transfer-freeze (FTF) technique used for microscopic observations (Hewes and Holm-Hansen, 1983). Particles are concentrated on a Nuclepore filter rather than glass fiber filter and then transferred to a microscope glass slide (Allali et al., 1995). The absorption spectrum of the particles is measured directly on the slide, and the pathlength amplification effect is avoided.

Measuring the absorption spectrum of suspended particles collected on a filter obviously overestimates $a_\phi^*(\lambda)$ to the extent that non-algal particles such as heterotrophic bacteria, zooplankton, and detritus contribute to light absorption. Several methods have been devised to correct for this problem. Chemical methods include washing the sample with a mixture of organic solvents, applying ultraviolet radiation in the presence of H_2O_2 (Konovalov and Bekasova, 1969), and bleaching the cells with peracetic acid (Doucha and Kubin, 1976) or NaOCl (Tassan and Ferrari, 1995). The chemical method most frequently used is that of Kishino et al. (1985). The filter is immersed in CH_3OH to extract alcohol-soluble pigments and the residual absorption measured on the bleached filter. $a_\phi^*(\lambda)$ is calculated from the difference between the absorption spectrum before and after bleaching. Allali et al. (1995, p. 1530) describe a modification of this procedure for measurements with the glass slide technique. The Kishino et al. (1985) method underestimates $a_\phi^*(\lambda)$ to the extent that $a_\phi^*(\lambda)$ includes contributions from

water-soluble pigments such as phycobilins and overestimates $a_\phi^*(\lambda)$ to the extent that methanol bleaching extracts detrital pheopigments and carotenoids (Sakshaug et al., 1997). An approximate correction for these effects can be made from knowledge of the detailed pigment composition (Bidigare et al., 1990a; Johnsen et al, 1994; Sosik and Mitchell, 1995). Ideally, $a_\phi^*(\lambda)$ should be partitioned into components from photosynthetic pigments, $a_{\mathrm{PS}}^*(\lambda)$, and nonphotosynthetic pigments, $a_{\mathrm{NPS}}^*(\lambda)$. Here again, an approximate partitioning can be made from knowledge of the detailed pigment composition.

ESTIMATION OF PHOTOSYNTHESIS

For purposes of estimating the parameters of P* vs. E_o curves, photosynthetic measurements are normally made using incubations that last no more than one hour. Although photosynthetic rates can theoretically be estimated from either O_2 production or CO_2 uptake, O_2 production methods, whether based on changes in O_2 concentration or the production of ^{18}O labeled O_2 from $H_2{}^{18}O$, are not sufficiently sensitive to provide reliable estimates of photosynthesis in oligotrophic environments after an incubation of only one hour, particularly in the light-limited portion of the P* vs. E_o curve (Williams, 1993). The ultimate precision of O_2 methods is probably 0.1-0.2 μmole O_2 L^{-1}.

The great appeal of estimating photosynthetic rates from the incorporation of ^{14}C-labeled inorganic carbon into organic carbon is the sensitivity of the method. As a somewhat extreme example, assume a P* of 0.1 g C g^{-1} chl *a* h^{-1} and a chl *a* concentration of 0.1 μg L^{-1}. The photosynthetic rate is therefore 0.01 μg C L^{-1} h^{-1}. At a dissolved inorganic carbon (DIC) concentration of 30 mg C L^{-1}, this photosynthetic rate would correspond to uptake of (0.01)/(30 ·

10^3) $\cong$ $3.3 \cdot 10^{-7}$ = 0.000033% of the DIC per hour. Since 1.0 Becquerel (Bq) = 1.0 disintegration per second or 60 disintegrations per minute (dpm), addition of 10^6 Bq of inorganic ^{14}C to a sample of such water would result (ignoring isotope discrimination) in the uptake of $(60)(3.3 \cdot 10^{-7})(10^6)$ = 19.8 dpm. Isotope discrimination (~4%) and counting efficiency on a liquid scintillation counter (~85%) would reduce the 19.8 dpm to (19.8)(0.85)/1.04 = 16 counts per minute (cpm). If the sample were counted for 60 minutes, the 95% confidence interval, assuming a Poisson distribution function for the counts, would be 6.4% of the count. 10^6 Bq of ^{14}C is an acceptable quantity of ^{14}C, and 6.4% is an acceptable counting precision. Thus the ^{14}C method does an admirable job of providing the sensitivity needed for characterizing P* vs. E_o curves.

What is being measured?

Sensitivity notwithstanding, there are a number of troublesome issues related to ^{14}C uptake measurements. Best known is the controversy over what ^{14}C-uptake measures (Peterson, 1980; Dring and Jewson, 1982). Experimental results usually indicate that the method measures something in excess of net photosynthesis (Steemann-Nielsen, 1955; Ryther, 1956). It is generally presumed that ^{14}C uptake estimates something between net and gross photosynthesis, although as noted by Falkowski and Raven (1997), the term "gross photosynthesis" should be reserved for oxygen evolution only. As a result of numerous studies since the development of the ^{14}C method almost 50 years ago (Steemann-Nielsen, 1952), it has become apparent that what the method measures depends on the physiological condition of the algae, the duration of the incubation, and whether or not the incubation spans a light:dark cycle (e.g., DiTullio and Laws, 1986). In incubations lasting no more than one hour, it is generally agreed that ^{14}C uptake

overestimates net photosynthesis, especially at irradiances near the compensation point (Dring and Jewson, 1982).

Production of $DO^{14}C$

A second troublesome issue is the loss of label from the particulate pool due to the release of labeled dissolved organic carbon (DOC) or heterotrophic respiration of ^{14}C-labeled organic matter. Release of labeled DOC can result from a variety of mechanisms, including excretion of glycolate due to photorespiration, exudation caused by the passive diffusion of DOC through the plasmalemma (Raven, 1993), spontaneous lysis of cells (von Boekel et al., 1992), lysis following viral attack (Cottrell and Suttle, 1995), and grazing ("sloppy feeding") by zooplankton (Roy et al., 1989). Analytical models suggest that such losses can substantially reduce the retention of ^{14}C in particulate matter in incubations lasting 12 hours or more when grazing rates are high and/or the phytoplankton community is dominated by small cells (Laws, 1984). However, similar reasoning suggests that in an incubation lasting only one hour the activity of $DO^{14}C$ would be no more than a few percent of particulate organic carbon (POC) activity. Models suggest that the specific activity of excreted DOC would be very low compared to the specific activity of inorganic carbon during the first hour of incubation, and this fact accounts for the small percentage of activity in the DOC pool.

These considerations are moot in the case of photosynthetrons, since the contents of each vial are acidified and degassed to drive off ^{14}C-labeled inorganic carbon rather than being filtered. The activity in the vials therefore represents the sum of POC and DOC activities. In the case of the radial photosynthetron, the entire volume of a 50-ml culture flask is filtered through a Whatman GF/F filter after an incubation of 20-120 minutes (Babin et al., 1994). Because the

incubations last no more than 2 hours, almost all the ^{14}C activity is expected to be in the POC (see above). An additional consideration is the fact that GF/F filters are known to adsorb $DO^{14}C$ (Maske and Garcia-Mendoza, 1994). In studies reported by Karl et al. (1998), for example, GF/F filters retained about half (46 ± 5%) of the $DO^{14}C$ activity that passed through 0.2 μm Nuclepore polycarbonate filters. To quantify adsorbed $DO^{14}C$ activity, Karl et al. (1998) found it necessary to store acidified filters in scintillation cocktail for roughly 10 days. The adsorbed activity is not efficiently detected in samples that are counted within one day following addition of scintillation cocktail. The increase in counts during the next 5-10 days is apparently due to desorption of the $DO^{14}C$ from the filters into the scintillation cocktail.

Sample volume

A typical scintillation vial can accommodate 20-25 ml of fluid, and in typical experiments, the volume of scintillation cocktail is 6-7 times the volume of water (e.g., Lewis et al., 1985b; Karl et al., 1998). This limits the volume of water in a conventional photosynthetron experiment to about 3 ml per vial. Virtually carrier-free ^{14}C stock solutions are commercially available, and in such solutions the specific activity of the ^{14}C is $1.85\text{-}2.29 \cdot 10^{12}$ Bq mol^{-1}. Addition of 10^6 Bq of inorganic ^{14}C from such a solution (see above) would imply the addition of 0.5 μmol of DIC. If the stock solution contained carrier-free DIC at a concentration of 2.5 mM (i.e., similar to the concentration of DIC in seawater), addition of 0.5 μmol of DIC would imply the addition of 0.2 ml of the stock solution. This is only about 7% of the volume of seawater in the scintillation vial, and of course the concentration of the DIC would be virtually unchanged. Thus, it is possible to carry out highly sensitive measurements with a conventional photosynthetron if one is willing to pay the price for carrier-free ^{14}C stock solutions.

One of the drawbacks of this approach is the possibility that the distribution of phytoplankton in the water may be patchy when subsampled on a scale of 3 ml. Thus even if the uptake of ^{14}C in each vial accurately reflects the photosynthetic rate in that vial, the patchy nature of the phytoplankton distribution may introduce noise into the P* vs. E_o plot. The radial photosynthetron addresses this problem by increasing the volume of seawater by more than an order of magnitude. Since carrier ^{12}C accounts for roughly 90% of the inorganic carbon in typical ^{14}C-stock solutions, this increase in volume facilitates the use of less expensive ^{14}C stock solutions with a specific activity of roughly $1.85 \cdot 10^{11}$ Bq mol^{-1}.

DO^{14}C in stock solution

An additional concern with respect to DO^{14}C is the presence of DO^{14}C in the stock solution. Since photosynthetic uptake after an incubation of no more than 1-2 hours will typically account for a very small fraction of the DI^{14}C, even a small amount of DO^{14}C in the stock solution can seriously bias results. This may be true even if samples are filtered through a GF/F filter because of the tendency of the filter to adsorb DOC. This is not a problem that can be effectively addressed after the fact. It is therefore necessary to ensure that the extent of DO^{14}C contamination is below the level that would cause trouble.

A simple first step is to add a known amount of ^{14}C stock solution to a scintillation vial, acidify the sample to drive off DI^{14}C, and count the activity that remains. The amount of ^{14}C added to the vial should be at least as great as the amount that will be added to the vials or culture flasks in the field, and the counts after acidification and degassing should be at the background level. If contamination is detected, the DI^{14}C can be purified by acidifying the stock

solution to drive off $^{14}CO_2$ and collecting the $^{14}CO_2$ in a basic medium. The purified stock should be checked to ensure that there is no detectable $DO^{14}C$ activity.

Incubation time

Incubation times in P* vs. E_o studies are kept short for two basic reasons. The first is acclimation. Phytoplankton acclimate to changes in environmental conditions such as irradiance, temperature, and nutrient concentrations. In some cases acclimation protects the cells from adverse conditions, e.g., the production of photoprotective pigments. In the absence of stress, acclimation leads to a balance between the light and dark reactions of photosynthesis while maximizing growth rate (Shuter, 1979). Because the irradiance experienced by cells growing on a light:dark (L:D) cycle is constantly changing, marine phytoplankton are themselves constantly acclimating to their environment, even when temperature and nutrient concentrations are constant. When the physiological condition of the algae is quantified by a metric such as the chl *a*/P700[4] ratio, light-shade acclimation is well described by a first-order rate constant of 0.02-0.06 h^{-1} (Falkowski, 1980). Hence during an incubation of one hour, the chl *a*/P700 ratio would be expected to change by no more than a few percent, and this would be a worst case scenario corresponding to a transition from very dim to very bright light or vice versa.

The molecular biological basis of acclimation seems to involve changes in the redox status of specific elements in the photosynthetic electron transport chain (Escoubas et al., 1995). The changes that occur tend to minimize the sensitivity of growth rate to changes in environmental conditions and in general influence either τ and/or σ_{PSII} in a way that causes E_k to be positively correlated with irradiance (Fig. 3). The xanthophyll cycle (Yamamoto and

[4] P700 is the reaction center chlorophyll of PSI. It is the primary electron donor of PSI. Peak absorbance is at 700 nm.

Chichester, 1965), for example, provides a mechanism for dissipating absorbed excitation energy thermally (Falkowski and Raven, 1997) and hence protects cells from photooxidative damage under high light conditions. The cycle involves conversion of an epoxidated xanthophyll, either diadinoxanthin or violaxanthin, to a de-epoxidated form, either diatoxanthin or zeaxanthin, respectively, in bright light. Quenching of excitation energy within the PSU antenna by the latter pigments reduces σ_{PSII}. Since $E_k = P_m^* / \alpha^* = 1/(\tau \sigma_{PSII})$, this acclimation to bright light increases E_k. In microalgae, the interconversion between the xanthophylls can occur on a time scale of 5-10 minutes (Falkowski and Raven, 1997). Of marine phytoplankton, only phycobilisome-containing species (Siefermann-Harms, 1985) and prochlorophytes appear to lack a xanthophyll cycle or analogue thereof.

The second reason for keeping incubation times short is concern over artifacts associated with containment in incubation vials. The artifacts fall into two general categories. The first is physiological damage to the cells associated with confinement. This can occur for a variety of reasons. For many years, there was great concern over metal contamination (Carpenter and Lively, 1980). Glass incubation bottles and/or ^{14}C stock solutions were implicated as the source of the metals (Fitzwater et al., 1982), and copper was generally suspected to be the metal responsible for adverse effects (Marra and Heinemann, 1987). To circumvent this problem, Fitzwater et al. (1982) proposed the use of so-called "clean" sampling and incubation protocols. However, Marra and Heinemann (1984) concluded that conventional incubation methodology alone did not necessarily depress photosynthetic rates. Subsequent studies (Marra and Heinemann, 1987; Williams and Robertson, 1989) clearly implicated sampling protocols rather than incubation methodology as the cause of contamination. The problem was traced to the central rubber cord and "O" rings of Niskin samplers and was solved by replacing the central

cord of neoprene or latex rubber with silicone or epoxy-coated stainless steel springs and the neoprene "O" rings with their silicone equivalents (Williams and Robertson, 1989). Alternatively, samples may be collected with GoFlo bottles, which do not have an internal closure.

The second category of artifacts is associated with the small size of incubation vials or bottles. Gieskes et al. (1979), for example, found that photosynthetic rates estimated in the North Equatorial Current from sunrise-to-sunset incubations in 30-ml and 300-ml bottles averaged 3% and 12%, respectively, of the corresponding values estimated from incubations in 3.8 liter bottles. In incubations conducted in 1.0 liter bottles, photosynthetic rates estimated from a series of 6 two-hour incubations were about 2.5 times the rate estimated from a single 12-hour incubation. Gieskes et al. (1979) suggested two possible explanations for their observations: (1) damage to organisms caused by collision with the glass walls of the incubation bottles (Verduin, 1960; Bender et al., 1987) and (2) lack of nutrient recycling in the smaller bottles due to the likely absence of relatively rare large zooplankton (Sheldon et al., 1973). They reasoned that the latter effect would be of little consequence in eutrophic waters, "where surplus nutrient is available for algal growth and rapid mineralization is not necessary to allow optimal growth" (Sheldon et al., 1973, p. 72-73).

In contrast to the Gieskes et al. (1979) results, Laws et al. (1987) found no bottle size effects on ^{14}C uptake when incubations were conducted in polycarbonate bottles ranging in size from 250 ml to 24 liters. Parallel incubations were conducted from sunrise to sunset and from sunrise to sunrise in the North Pacific subtropical gyre. Whether the difference in the results of Gieskes et al. (1979) and Laws et al. (1987) reflects the use of glass bottles in the former study

and polycarbonate bottles in the latter study is unclear. In any case, there are no reports of bottle size effects on ^{14}C uptake involving incubations shorter than two hours.[5]

Patchiness

A concern related to bottle size effects is patchiness. Patchiness in the distribution of phytoplankton occurs over a wide range of spatial scales (Kierstead and Slobodkin, 1953; Cassie 1959a,b; Platt, 1972; Silver et al., 1978; Davis et al., 1992; Yoder et al., 1994; Allen et al., 1996; Blackburn et al., 1998). Biological variability at the 30-liter (Niskin bottle) scale has been observed (Davis et al., 1992). Replication of chlorophyll measurements at oligotrophic oceanic sites was poorer when subsamples of 130 ml were drawn directly from the Niskin bottle (coefficient of variation (CV) = 11.6%) than when the subsamples were taken from a carboy with mixed water from one Niskin bottle (CV = 4.5%) (Venrick et al., 1977). To minimize scatter caused by patchiness, subsamples should therefore be taken from samples mixed from one Niskin bottle to reduce the within-sample variability due to subsampling (Venrick, 1971).

Curve fitting

Several problems emerge when equations 4-8 are fit to field data. First, which equation should be used? Second, what is the best way to estimate α^* and P_m^*? Equations 4-5 and 7-8 all merge in the limits as $E_o/E_k \rightarrow 0$ and $E_o/E_k \rightarrow \infty$. However, there are considerable differences in the values of the functions at intermediate E_o/E_k values. Thus even if accurate values of α^* and P_m^* are determined, estimates of integral photosynthetic rates may differ by as much as a factor of 5 (Frenette et al., 1993), depending on which model is used for integration purposes. Given

[5] However, Bender et al. (1987) report that *Gymnodinium* and *Pedinella* can rapidly lose their flagellae by colliding with walls of glass containers

equal values of α^* and P_m^*, the hyperbolic tangent will give the lowest areal photosynthetic rate and the piecewise linear function the highest.

The sensitivity of calculated areal photosynthetic rates to model formulation stems in part from the procedures that have been used to estimate α^* and P_m^*. For example, if α^* and P_m^* are chosen so that the model fits the experimental data in the limit of low and high irradiance, then the calculated areal photosynthetic rate will be sensitive to the choice of model, but the values of α^* and P_m^* will not. On the other hand, if α^* and P_m^* are chosen to give a good fit to results at all irradiances, the calculated values of α^* and P_m^* will become sensitive to the choice of model, but the calculated areal photosynthetic rates will not. The usual procedure is to determine α^* and P_m^* by least squares, specifically by minimizing the sum of the squared deviations of the measured P^* from the value of P^* calculated using one of equations 4-8 (Frenette et al., 1993). We will call the latter $\hat{P}^*$. This procedure seems intuitively reasonable, but it is not the best approach to take if the goal is to minimize uncertainty in the estimate of areal production.

The areal photosynthetic rate **P** is given by the equation

$$\mathbf{P} = \int_0^{Z_m} \mathrm{chl}(z) P^*(E_o(z))\,dz \qquad (15)$$

where chl(z) is the chlorophyll concentration at depth z and the integration extends from the surface to depth Z_m, usually the depth of the euphotic zone. For the sake of simplicity, we will assume that the chlorophyll concentration is independent of depth. In that case,

$$\mathbf{P} = \mathrm{chl} \int_0^{Z_m} P^*(E_o(z))\,dz = \mathrm{chl}\ \mathbf{P}^* \qquad (16)$$

Where chl is the constant chlorophyll concentration and **P*** is the integral of P*. If E_o decays in an exponential manner with depth, then $E_o = E_{os}e^{-kz}$, where E_{os} is the irradiance at the surface, and $dE_o/dz = -kE_o$. It is then straightforward to show that

$$\mathbf{P^*} = \frac{1}{k}\int_{E_{om}}^{E_{os}} \frac{P^*(E_o)}{E_o} dE_o \tag{17}$$

where E_{om} is the irradiance at depth Z_m and E_{os} is the irradiance at the surface. If $P^*(E_o)$ is known at a series of N discrete values of E_o over the interval [E_{om} E_{os}], the integral in equation 17 can be approximated by the expression (Laws, 1997)

$$\int_{E_{om}}^{Eos} \frac{P^*(E_o)}{E_o} dE_o \cong \sum_{n=1}^{N} W_n \frac{P^*(E_{on})}{E_{on}} \tag{18}$$

where E_{on} is an abscissa of the numerical integration scheme and W_n is the associated weight. Hence, if the goal of curve fitting is to provide an accurate estimate of the areal photosynthetic rate, the least squares procedure for determining α^* and P_m^* should seek to minimize

$$\sum_{n=1}^{N}\left(\frac{W_n}{E_{on}}\right)^2\left(P_n^* - \hat{P}_n^*\right)^2 \tag{19}$$

where P_n^* and $\hat{P}_n^*$ equal $P^*(E_{on})$ and $\hat{P}^*(E_{on})$, respectively. In a case, for example, where the abscissas (E_{on}) correspond to the midpoints of a series of irradiance intervals of equal length, all the W_n are equal, and the least squares procedure would seek to minimize

$$\sum_{n=1}^{N}\left(\frac{P_n^* - \hat{P}_n^*}{E_{on}}\right)^2 \tag{20}$$

This is quite different from the usual least squares, which would seek to minimize

$$\sum_{n=1}^{N}\left(P_n^* - \hat{P}_n^*\right)^2 \tag{21}$$

Fig. 4 illustrates the nature of the problem that (20) seeks to address. Calculating areal production amounts to carrying out an integration over depth. Because irradiance decays more-or-less exponentially in the water column, equal intervals of irradiance do not correspond to equal depth intervals. If light decays exponentially and if the euphotic zone is defined to be the water column above the 1% light level, then half the euphotic zone lies below the 10% light level. The areal production calculation can be carried out explicitly by calculating the appropriate integral over depth. The same result can be obtained by carrying out the integration over irradiance space, but weighting the observations according to the inverse of the irradiance, i.e., equation 17.

The implication is that a least-squares procedure designed to give accurate estimates of areal production would amount to a weighted least squares in which more weight was assigned to P* values measured at low irradiances. As a first approximation, using (20) as a least-squares criterion would be much preferable to (21). The fact that criteria other than the minimization of (20) have routinely been used to determine α^* and P_m^* undoubtedly accounts for some of the sensitivity of calculated areal photosynthetic rates to the choice of analytical models (Frenette et al., 1993). The importance of weighting observations according to the inverse of the irradiance reflects the fact that, “Photosynthesis normally takes place at nonsaturating irradiances . . and . . irradiances over most of the euphotic zone are nonsaturating” (Frenette et al., 1993, p. 684). While it is tempting to think that α^* should be determined from data collected at low light and P_m^* from data collected at high light, choosing the parameters in this way makes integral production very sensitive to the choice of analytical model (Fig. 2 and Frenette et al., 1993).

If the vertical distribution of chlorophyll is taken into account in the least-squares procedure, the existence of a deep chlorophyll maximum will cause even more weight to be

assigned to P* measured at low irradiance. The analogue of equation 15 in the case of a depth-dependent chlorophyll concentration is

$$\mathbf{P} = \frac{1}{k}\int_{E_{om}}^{E_{os}} chl(\ln(E_{os}/E_o)/k)\frac{P^*(E_o)}{E_o}dE_o \cong \sum_{n=1}^{N} W_n chl(Z_n)\frac{P^*(E_{on})}{E_{on}} \quad (22)$$

where $Z_n = \ln(E_{os}/E_{on})/k$. The least squares procedure in this case seeks to minimize

$$\sum_{n=1}^{N}\left(\frac{W_n chl(Z_n)}{E_{on}}\right)^2\left(P_n^* - \hat{P}_n^*\right)^2 \quad (23)$$

Given the E_{on} for n = 1:N, the weights W_n are determined by requiring that the numerical integration scheme in equations 18 and 22 be able to exactly integrate any polynomial in E_o of order < N on the interval [E_{om} E_{os}]. This condition is analogous to the constraint imposed to determine the weights in Gauss quadrature and the more general method of moments (Laws, 1997). In the case of N = 3, for example, the constraint equations are as follows:

$$W_1 + W_2 + W_3 = E_{os} - E_{om}$$

$$W_1E_{o1} + W_2E_{o2} + W_3E_{o3} = \frac{E_{os}^2}{2} - \frac{E_{om}^2}{2}$$

$$W_1E_{o1}^2 + W_2E_{o2}^2 + W_3E_{o3}^2 = \frac{E_{os}^3}{3} - \frac{E_{om}^3}{3}$$

Since the constraint equations are linear with respect to the W_n, they can easily be solved using matrix algebra.

If any one of equations 4-8 is fit to experimental data, the analytical function will automatically equal 0 at $E_o = 0$. However, uptake of ^{14}C can occur in the dark as a result of anaplerotic metabolism and chemosynthesis, and dark uptake of ^{14}C is a common observation in ^{14}C incubations (Li, 1987; Taguchi et al., 1988). In low-latitude open-ocean waters and toward the base of the euphotic zone, dark ^{14}C uptake can constitute a large percentage of light uptake

(Saijo and Takesue, 1965; Morris et al., 1971; Taguchi, 1983). The phenomenon is especially common in tropical and subtropical plankton less than 1.0 μm in size (Li et al., 1983; Herbland et al., 1985).

Li (1987) has provided a good review and discussion of dark $^{14}CO_2$ uptake. While careful not to rule out any of the possible explanations for this phenomenon, he seemed to favor uptake by heterotrophic bacteria as the most likely mechanism. Whatever the cause, dark uptake of $^{14}CO_2$ is obviously the result of nonphotosynthetic processes (Legendre et al., 1983), and a correction for dark uptake should be made in the analysis of P* vs. E_o curves. The most common procedure is to carry out parallel incubations in the light and dark and subtract dark uptake from light uptake. The P* vs. E_o curve fit to the resultant data is forced through the origin (i.e, equations 4-8). An alternative approach is to include an intercept in equations 4-8 and determine the value of the intercept by least squares (Suggett et al., 2001).

COMPLEMENTARY METHODS

Variable fluorescence

Two general categories of analytical tools may be used to complement information obtained from P* vs. E_o studies. The first makes use of the variable fluorescence yield of PSII (Falkowski and Kiefer, 1985) to obtain estimates of parameters such as σ_{PSII} and τ and to provide an independent estimate of E_k and P_m^*. Given the theoretical analysis presented by Kolber and Falkowski (1993), it is straightforward to show that:

$$q_P = \frac{E_k}{E_o} f(E_o / E_k) \tag{24}$$

where q_P is the fraction of open reaction centers at irradiance E_o and f, as explained above, is a dimensionless function equal to P^*/P^*_m. The value of q_P can be calculated from the change in fluorescence yields of probe flashes preceding or following a saturating pump flash as follows:

$$q_p = (F'_m - F')/(F'_m - F'_o) \quad (25)$$

where F' and F'_m are the fluorescence yields induced by a weak probe flash preceding and immediately following the pump flash, respectively, measured under ambient light (E_o), and F'_o is the fluorescence yield induced by a weak probe flash in a situation when all PSII reaction centers are open, i.e., following 1-2 seconds of dark acclimation (Kolber and Falkowski, 1993). The value of E_k is determined using standard least squares after choosing the appropriate $f(E_o/E_k)$ from equations 4-8. For example, in the case of the rectangular hyperbola (equation 4), $f(E_o/E_k) = (E_o/E_k)/(1+E_o/E_k)$ and $q_P = 1/(1+E_o/E_k)$. Figure 5 shows the dependence of q_P for the five models defined by equations 4-8. The value of q_P at $E = E_k$ varies from 0.5 for the rectangular hyperbola to 1.0 for the piecewise linear model. To be consistent, comparisons of E_k values derived from P* vs. E_o and q_P vs. E_o curves should be based on the same analytical model. Figure 6 illustrates the nature of the problem. In this case, q_p experimental data have been fit by least squares to four analytical models. The negative exponential and rectangular hyperbola formulations give the best fit to the q_p data, and the goodness of fit is very similar in these two cases. Nevertheless, the calculated E_k values differ by a factor of 1.6.

Significant differences in parameter values may also arise if the least-squares procedures used to determine the parameter values weight observations in fundamentally different ways. Expression (20), for example, assigns a similar weight to observations as does the right-hand side of equation 24. However, expression (21) weights observations differently than equation 24.

This problem may account for some of the reported inconsistencies in E_k values derived from ^{14}C-based and fluorescence-based methods (Hartig et al., 1998).

The value of σ_{PSII} can be estimated by gradually increasing the intensity of the pump flash and following the flash-intensity saturation curve of variable fluorescence (Kolber and Falkowski, 1993). Assuming that this curve can be described by a cumulative one-hit Poisson function, it follows that:

$$(F - F_o)/(F_m - F_o) = 1 - \exp(-\sigma_{PSII} J) \quad (26)$$

where F_o and F_m are in vivo fluorescence yields induced by a weak probe flash in the dark (initial) and following a saturating flash (maximal), respectively, measured in dark-acclimated cells, and F is the fluorescence yield immediately (1-100 μs) following a pump flash of energy J (n.b., $F_o < F < F_m$). In estimating σ_{PSII} from equation 26, care must be taken to correct for the spectral characteristics of the blue light-emitted diodes (LEDs) of the fast-repetition-rate fluorometer (FRRF), which have a peak excitation at 478 nm with a 30 nm half bandwidth (Suggett et al., 2001). This may be done by using equation 1 to calculate the ratio of $\overline{a_\phi^*}$ for the LEDs and submarine irradiance field and dividing the value of σ_{PSII} determined from equation 26 by that ratio. Once E_k and σ_{PSII} have been determined, τ can be calculated from the equation $\tau = 1/(\sigma_{PSII} E_k)$. Given τ, P_m^* can be calculated from equation 9.

Instruments designed to facilitate these measurements include the pump-and-probe fluorometer or PPF (Kolber et al., 1988), the fast-repetition-rate fluorometer or FRRF (Greene et al., 1994), and the pulse-amplitude modulated-fluorescence meter or PAM (Buechel and Wilhelm, 1993; Hartig et al., 1998). In the PPF technique, fluorescence from a weak probe flash is measured before (F_o) and 80 μs after (F_m) a short (5-μs half-width) actinic pump flash. The

FRRF fluorometer generates a series of 32-64 excitation flashlets, each with a 1-µs half-width, at a repetition rate of 100-200 kHz. The FFR significantly shortens the experimental protocol compared to the PPF and increases the signal-to-noise ratio (Greene et al., 1994). One of the great appeals of fluorescence-based techniques is that they do not involve incubations and hence eliminate potential artifacts associated with sample confinement for other than a very brief period.

Oxygen-based methods

The second general category of complementary techniques involves measurement of gross production and respiration using oxygen. Because oxygen-based methods are less sensitive than ^{14}C-based methods, longer incubation times are required. The advantages include minimal ambiguity with respect to what is being measured and the ability to calculate respiration in both the light and dark.

For many years, oxygen-based techniques relied on the so-called oxygen light-and-dark bottle method (Williams et al., 1979) in which parallel incubations are conducted in clear (light) and opaque (dark) bottles. Gross photosynthesis is equated to the difference in oxygen concentrations in the light and dark bottles at the end of the incubation. Respiration is equated to the difference in oxygen concentrations in the dark bottle between the beginning and end of the incubation. The calculation of gross photosynthesis in this way requires assuming that respiration rates are the same in the light and dark bottles.

To avoid the assumption that respiration rates are identical in the light and dark, Grande et al. (1982) developed an oxygen-based method for estimating gross photosynthesis based on the production of ^{18}O-labeled O_2 from $H_2{}^{18}O$. Although the ^{18}O method clearly estimates the rate

of O_2 production by PSII, there is no guarantee that all O_2 produced by PSII will diffuse into the surrounding seawater, and not all O_2 produced by PSII is linked to electron transport from water to CO_2, i.e., carbon fixation. In the Mehler reaction, an O_2 molecule is generated by the oxidation of water on the donor side of PSII, and a second O_2 molecule is reduced on the reducing side of PSI. This so-called pseudocyclic electron transport may be coupled to generation of ATP, or it may be a mechanism to alleviate the potentially damaging effects of high rates of light absorption by PSII (Falkowski and Raven, 1997). Because a molecule of labeled O_2 is produced and a molecule of unlabeled O_2 consumed, the Mehler reaction is recorded as gross photosynthesis by the ^{18}O method. In the ^{18}O method, the Mehler reaction probably accounts for ~10% of ^{18}O-labeled O_2 (Laws et al., 2000).

Comparisons between results obtained using ^{14}C and oxygen-based methodologies and between light-and-dark bottle and ^{18}O methodologies provide insights concerning our understanding of the photosynthetic process and the ecology of phytoplankton. With few exceptions, most studies indicate that the ratio of oxygen-based gross production to ^{14}C-based photosynthesis lies in the range 1.5-2.5 when incubations last 4 hours or longer (Table 1). The fact that the ratio is greater than 1.0 reflects a combination of the Mehler reaction, photorespiration, excretion, and mitochondrial respiration (Bender et al., 1999) and the fact that the PQ lies in the range 1.1-1.4 (Laws, 1991; Williams and Robertson, 1991).

Since most ^{14}C-based estimates are based on filtered samples, ^{14}C-labeled DOC may account for a substantial fraction of ^{14}C fixation. In one of two mesocosm studies reported by Bender et al. (1987), for example, total ^{14}C counts (POC + DOC) exceeded POC activity by almost 30% after an incubation of only 4 hours and by 40% after 8 hours. This phenomenon is likely to be most significant in phytoplankton communities dominated by small cells (see above).

For example, the (gross O_2)/(^{14}C uptake) ratio of 1.5 reported for *Synechococcus* by Grande et al. (1991) can be largely explained by excretion (factor of 1.3) combined with a PQ of 1.1[6], i.e., (1.3)(1.1) = 1.43.

In general, one would expect the (gross O_2)/(^{14}C uptake) ratio to increase with time as the recently fixed ^{14}C finds its way into respiratory substrates. In general this is true, but the decline in particulate ^{14}C activity during the night in 24-hour incubations is not always as great as one would expect, and in some cases particulate counts actually increase (Taguchi et al., 1988; Allen et al., 1996). DiTullio and Laws (1986) speculate that at least some of the nocturnal increase in particulate ^{14}C counts during 24-hour incubations reflects incorporation of ^{14}C-labeled DOC excreted during the previous photoperiod. The implication of the results summarized in Table 1 is that after incubations of 4 hours or longer, the (gross O_2)/(^{14}C uptake) ratio will substantially exceed the likely value of the associated PQ (i.e., 1.1-1.4), especially if ^{14}C uptake is calculated from particulate ^{14}C counts. This fact provides further motivation for keeping P* vs. E_o incubations as short as possible and for including both dissolved and particulate ^{14}C counts in the calculations.

Table 2 provides a comparison of gross photosynthetic rates estimated from the production of ^{18}O-labeled O_2 from $H_2{}^{18}O$ and from light-and-dark bottle incubations. The fact that the two estimates are not identical is normally attributed to differences in the rates of light and dark respiration, although as noted, the Mehler reaction causes the ^{18}O method to overestimate gross photosynthesis. In most cases the ^{18}O estimate is higher, but this is not always the case. The most extreme ratios occur when net O_2 production is negative. Under those conditions, apparent differences in the rates of light and dark respiration become magnified in

[6] The culture was undoubtedly grown in an ammonium-based medium, since *Synechococcus* lacks nitrate reductase.

the comparison of gross photosynthetic rates. Mathematically, the ratio of ^{18}O-based gross photosynthesis to light-and-dark bottle gross photosynthesis can be written as (NP + LR)/(NP + DR), where NP is net O_2 production, and LR and DR are the light and dark respiration rates[7], respectively. The ^{18}O method measures the sum of NP and LR, while the light-and-dark bottle method measures NP and DR separately. If NP is negative, it is straightforward to show that (NP + LR)/(NP + DR) will exceed LR/DR if LR/DR > 1 and will be less than LR/DR if LR/DR < 1. The opposite is true if NP is positive.

Respiration rates measured in the dark are known to be positively correlated with the growth rates of microalgae (Laws and Bannister, 1980; Falkowski and Raven, 1997, Fig. 8.5). Furthermore, if a microalga is grown at an irradiance that is subsaturating with respect to photosynthesis and then exposed to higher light, the initial respiration rate after subsequently placing the culture in the dark is enhanced relative to the dark respiration rate measured immediately after exposure to the subsaturating irradiance (Falkowski and Raven, 1997). Given these observations and current understanding about the role of respiration in biosynthesis, it would seem reasonable to expect that light respiration rates would be positively correlated with gross photosynthesis. However, comparisons of light respiration rates with ^{18}O-based photosynthetic rates show very little correlation between the two. In the experiments summarized in Fig. 7, for example, only the data for *Synechococcus bacillaris* show a statistically significant positive correlation ($r = 0.83$, $p < 0.01$). The correlation coefficients in the case of the three Bedford Basin experiments range from 0.22 to 0.26. Furthermore, even in the case of the *S. bacillaris* culture, the light respiration rate increases by less than a factor of 2 while gross O_2 production increases by more than a factor of 6. Although in some cases light respiration rates

[7] LR in this context is an apparent light respiration rate. It includes the effects of the Mehler reaction and is calculated as the difference between the ^{18}O estimate of gross photosynthesis and the light-and-dark bottle estimate of net O_2 production.

have been estimated to be as much as 3-8 times greater than dark respiration rates (Bender et al., 1987; Grande et al., 1991), there is often little difference between the two. For example, dark respiration rates reported by Grande et al. (1989, Table 1) exceed light respiration rates in 4 of 9 cases. A likely explanation for the similarity of light and dark respiration rates and the lack of correlation between light respiration rates and gross O_2 production is that most respiration in field samples is due to heterotrophs. The counter to this argument would seem to be the *Synechococcus* culture results in Fig. 7. At similar rates of gross photosynthesis, light respiration was consistently higher for this culture than for the Bedford Basin samples. However, net O_2 production by the *Synechococcus* culture was actually negative in 9 of 13 cases. The culture may have been contaminated with heterotrophic bacteria.

FROM P* VS. E CURVES TO AREAL PHOTOSYNTHETIC RATES

As previously noted, areal productivity **P** is the integral over depth of the product of the chlorophyll concentration and P* (Eq. 15). Assuming that irradiance decays in an exponential manner with depth, areal productivity can be equivalently expressed as 1/k times the integral over irradiance of the product of the chlorophyll concentration and P^*/E_o (Eq. 22). The latter representation of **P** is a convenient formulation for comparison with P* vs. E curves. Because the integrand in equation 22 is the product of P* and the quotient of the chlorophyll concentration and E_o, choosing parameter values (e.g., α and P_m) that give the best fit to P* vs. E data will virtually never give the best estimate of the areal photosynthetic rate. Assuming that estimating areal photosynthetic rates is the goal of the curve fitting exercise, the resolution of this problem is to carry out a least squares in which the parameters are chosen to minimize

$\sum_{k=1}^{N}\left[W_k\left(\frac{chl}{E_o}\right)_k\left(P_k^* - \hat{P}_k^*\right)\right]^2$ rather than $\sum_{k=1}^{N} W_k^2\left(P_k^* - \hat{P}_k^*\right)^2$. Assuming that a least-squares procedure is carried out on the correct function, the calculated areal photosynthetic rate will be relatively insensitive to the analytical expression used to describe P*. Figure 8 shows four functions fit to noise-corrupted P^*/E_o data in which the underlying functional relationship is $P^*(x) = 1 - e^{-x}$. When $\hat{P}^*$ is assumed to equal $1 - e^{-x}$, the analytical function accounts for 99% of the variance in the data. However, a hyperbolic tangent or rectangular hyperbola gives almost as good a fit (98% of variance accounted for). Only the piecewise linear function (Fig. 8A) gives a significantly poorer fit (91% of variance accounted for). However, in order to compensate for the wrong choice of analytical expression, biased values must be assigned to parameters. In Fig. 8, for example, the values of P_m^* and E_k used in the simulation were 10 and 100, respectively. The least squares value of E_k in Fig. 8D is 122. The large value of E_k in Fig. 8D compensates for the fact that $1/(1 + x) < (1 - e^{-x})/x$ for all values of x between 0 and ∞ (Fig. 2). In order to minimize the sensitivity of calculated areal photosynthetic rates to the choice of analytical function used to describe P* and to the choice of parameter values (i.e., E_k and P_m^*), it is important to apply least-squares procedure in a way that minimizes the errors in the estimated values of the integrand used to calculate **P**. The appropriate expression to minimize is $\sum_{k=1}^{N}\left[W_k\left(\frac{chl}{E_o}\right)_k\left(P_k^* - \hat{P}_k^*\right)\right]^2$. Obviously, this approach tends to put more weight on observations made at lower irradiances than would be the case if the parameters were chosen so as to minimize $\sum_{k=1}^{N} W_k^2\left(P_k^* - \hat{P}_k^*\right)^2$.

SENSITIVITY OF AREAL PRODUCTIVITY ESTIMATES TO α^* AND P_m^*

All of the functions defined by equations 4-8 have the form $P^* = P_m^* f(\alpha^* E_o / P_m^*)$. For such functions, it is straightforward to show that

$$(P_m^*/P^*)(\partial P^*/\partial P_m^*) + (\alpha^*/P^*)(\partial P^*/\partial \alpha^*) = 1 \qquad (27)$$

The first term in this equation is the ratio of the percent change in P* caused by a small percent change in P_m^*, and the second term is the ratio of the percent change in P* caused by a small percent change in α^*. The sum of these two ratios must equal 1 in the limit of very small percent changes in P_m^* and α^*. In other words, if a 4% increase in P_m^* produces a 1% increase in P*, then a 4% increase in α^* will produce approximately a 3% increase in P*, since the sum of the ratios of the percentage changes must equal 1 in the limit of very small changes in P_m^* and α^*. Equation 27 will remain true even if P* is integrated over depth and/or time, because in such cases the order of integration and differentiation (with respect to P_m^* and α^*) can be interchanged. Furthermore, it is also true for P, i.e., it is true if P* is multiplied by the chlorophyll concentration. Thus, for example, equation 27 is true if P* is the photosynthetic rate per unit chlorophyll at a given depth and time, and it is also true for P, **P** and **P***.

The sensitivity of estimates of daily areal production to α^* and P_m^* can be easily ascertained in the case of a well-mixed system if α^* and P_m^* are assumed to be constant, independent of depth and time of day. The nature of the sensitivity will depend systematically on which of equations 4-8 is used to describe the P* vs. E_o relationship, on the depth of the mixed layer, and on the relationship between E_k and the average irradiance in the mixed layer. For

purposes of integrating over time, it is convenient to assume that E_o increases in a linear manner from zero at sunrise to a maximum at midday and declines in a linear manner to zero at sunset. Given that assumption, any of the five models can easily be integrated over time. For example, in the case of the hyperbolic tangent, the average P* during the photoperiod is $[P_m^{*2}/(\alpha^* E_m)]\ln[\cosh(\alpha^* E_m / P_m^*)]$, where E_m is the midday irradiance.

The integration over depth is performed by assuming that irradiance decays exponentially in the water column, i.e., $E = E_{os}e^{-kZ}$, where E_{os} is the irradiance just below the surface, Z is depth, and k is the vertical attenuation coefficient. For mathematical simplicity, it is convenient to formulate the depth integrations in terms of a dimensionless dummy variable kZ and to examine the results in terms of the dimensionless optical depth of the mixed layer, kD, where D is the depth of the mixed layer. The depth integration must be handled numerically in the case of the hyperbolic tangent and rectangular hyperbola. However, the numerical integrations are straightforward for reasonable values of the optical depth, since the integrands are well-behaved mathematically. Because the exponential function has an absolutely convergent power series expansion, the depth integrations can be carried out analytically in the case of the negative exponential model, but the result takes the form of an infinite series (e.g., Lewis et al. 1985b). However, the series has good convergence properties. Alternatively, the negative exponential model can be integrated numerically over depth. With the foregoing assumptions, the piecewise-linear model can be analytically integrated over both depth and time, but the results depend on the relationship between E_k, E_{omid}, and $E_{omid}e^{-kD}$, where E_{omid} is the midday irradiance just below the surface. If $E_k > E_{omid}$, then according to the piecewise-linear model photosynthesis is light-limited even at the surface at midday. In that case P* is independent of P_m^* at all times and depths and depends entirely on α. If $E_{omid}e^{-kD} < E_k < E_{omid}$, then at midday photosynthesis is

light-saturated near the surface and light-limited near the base of the euphotic zone. In that case the ratio $[(P_m^*/\mathbf{P^*})(\partial\mathbf{P^*}/\partial P_m^*)]/[(\alpha^*/\mathbf{P^*})(\partial\mathbf{P^*}/\partial\alpha^*)] = (2x \ln(x) - 2x + 2)/(2x - 1 - x^2y)$, where $x = E_{omid}/E_k$, $y = e^{-kD}$, and **P*** is the integral of P* over the photoperiod and the depth of the mixed layer. If $E_k < E_{omid}e^{-kD}$, then photosynthesis is light-saturated throughout the mixed layer at midday, and $[(P_m^*/\mathbf{P^*})(\partial\mathbf{P^*}/\partial P_m^*)]/[(\alpha^*/\mathbf{P^*})(\partial\mathbf{P^*}/\partial\alpha^*)] = (2y - 2xy \ln(y) - 2)/(1 - y)$.

The ratio $[(P_m^*/\mathbf{P^*})(\partial\mathbf{P^*}/\partial P_m^*)]/[(\alpha*/\mathbf{P^*})(\partial\mathbf{P^*}/\partial\alpha*)]$ is shown in Fig. 9-10 for the five P* vs. E_o functions defined by equations 4-8 as a function of the optical depth of the mixed layer. In Fig. 9, the average irradiance in the mixed layer was 20% of E_k, and in Fig. 10, the average irradiance in the mixed layer was 3 times E_k. Given the assumptions of the model, the average irradiance in the mixed layer equals $(E_{omid}/2)(1 - e^{-kD})/(kD)$. For optical depths < 6, **P*** is substantially more sensitive to α^* than to P_m^* for all five models when the average irradiance in the mixed layer equals $E_k/5$. Under these assumed conditions, **P*** is most sensitive to α* for the piecewise-linear model and least sensitive for the rectangular hyperbola model. If the average irradiance in the mixed layer equals $3E_k$, **P*** is much more sensitive to P_m^* than to α^*. Under these assumed conditions, **P*** is most sensitive to P_m^* for the piecewise-linear or light-inhibited models and least sensitive for the rectangular hyperbola model. It is apparent from an examination of Fig. 9-10 that the differences in the sensitivity of the five models to P_m^* and α^* are most pronounced for shallow optical depths. It is also apparent from these figures that the relative sensitivity of **P*** to P_m^* and α^* depends very much on the relationship between E_k and the average irradiance in the mixed layer.

RELATIONSHIP BETWEEN E_K AND IRRADIANCE

Sakshaug et al. (1997, p. 1657) have argued that, "Phytoplankton strive to maintain an optimum balance between light and dark reactions of photosynthesis . . . . This balance occurs at the irradiance indicated by the light saturation parameter, E_k." Actually, this "optimum" balance is never achieved, because the rate of the light reactions never increases in direct proportion to irradiance until $P^* = E_k\alpha^* = P_m^*$. The reason reflects the requirement to balance the rates of the light and dark reactions of photosynthesis. According to Shuter's (1979) microalgal growth model, for example, the sum of the fractions of cell carbon allocated to the light and dark reactions of photosynthesis, R_L and R_D, respectively, is a constant, C, under light-limited growth conditions. Shuter assumes that the rate of the dark reactions is proportional to R_D and that the rate of the light reactions is proportional to the product of R_L and E_o. For growth rate to increase by a factor f, R_D must therefore increase by a factor f, and R_L must become $C - fR_D$. In order for the rate of the light reactions to increase by a factor f, the irradiance must therefore increase by a factor of $fC/(C - fR_D) = f/(1 - fR_D/C)$. When $R_D << C$, growth rate is almost directly proportional to E_o. However, since $f/(1 - fR_D/C) > f$, E_o must always increase by more than a factor f to make the growth rate increase by a factor f. Furthermore, the requirement for balanced growth means that the cell cannot keep R_L constant in the light-limited region of the growth rate-irradiance curve.

Babin and Morel have studied the relationship between E_k and average mixed layer irradiance using data collect from the Eastern Mediterranean, Atlantic, and Pacific oceans. Their results show that E_k is highly correlated with the average mixed layer irradiance, and about 80% of their data lie within an envelope defined by $\overline{E}_o/E_k = 2\text{-}4$, where $\overline{E}_o$ is the average mixed layer irradiance (Fig. 3). $\overline{E}_o$ was greater than E_k in every case but one. Fig. 10 would thus appear

quite relevant to field data. The implication is that within the mixed layer estimates of areal production will be more sensitive to P_m^* than to α^*. A corollary conclusion is that estimates of total water column production will be more sensitive to α^* than to P_m^* only when the mixed layer is optically shallow, much of the production occurs below the mixed layer, and photosynthesis below the mixed layer is light limited (e.g., E_k at each depth is greater than the average irradiance at that depth). Morel et al. (1996) provide a good example of this situation at their oligotrophic site off the northwest African coast, where the euphotic zone extended below the depth of the mixed layer and light-limited production accounted for at least half of total production. However, at their mesotrophic and eutrophic sites, where the euphotic zone was relatively shallow and well mixed, calculated areal production was about twice as sensitive to P_m^* as to α^*.

Why does E_k tend to be roughly 25-50% of the mean mixed layer irradiance? Most models of phytoplankton growth assume that phytoplankton acclimate to environmental conditions in a way that maximizes growth rate (e.g., Shuter, 1979). If equation 8 describes the relationship between irradiance and photosynthetic rate, then growth rate is maximized as long as $E_k \leq E_o$. However, for equations 4, 5, and 7, the photosynthetic rate is maximized only in the limit as $E_o/E_k \rightarrow \infty$, and for equation 6 with b = 0.03, photosynthetic rate peaks at E_o/E_k = ln(1.03/.03) = 3.5. Hence with the exception of the piecewise linear model, the model equations imply that growth rate is maximized only when E_o/E_k is substantially greater than 1. Geider et al. (1998, p. 679) have commented, “Acclimation may also serve to limit the damage that may be incurred as a consequence of exposure to adverse environmental conditions.” The data in Fig. 3 are in fact consistent with photoacclimation involving “a tradeoff between maximizing growth at low irradiance vs. minimizing the potential for photo-oxidative damage at high irradiance”

(Geider et al., 1998, p. 680). With b = 0.03, equation 6 implies that growth rates will be close to maximum when E_o/E_k lies in the range 2-4 (Fig. 2). The field data are consistent with this model if one assumes that phytoplankton acclimate so as to achieve close-to-maximum photosynthetic rates within a range of irradiances centered on the mean irradiance in the mixed layer.

Not all studies have concluded that errors in P_m^* affect estimates of areal photosynthetic rates more than equivalent relative errors in α^*. Lewis et al. (1985b), for example, reached exactly the opposite conclusion. However, their conclusion was not based on simultaneous measurements of E_o and E_k, but rather on a reported mean E_k of 52 W m^{-2} and the assumption [based on data reported by Reed (1977)] that E_{os} < 150 W m^{-2}. They concluded that $E_{os}/E_k < 4$ for much of the ocean. Given this conclusion, their analysis, based on a formulation identical to equation 5 for P* vs. E_o, indicated that areal production would be more sensitive to α^* than P_m^*.

The value of 52 W m^{-2} for E_k cited by Lewis et al. (1985b) is equivalent to about 250 μmol quanta m^{-2} s^{-1} of PAR (Strickland, 1958). This is about 60% greater than the mean E_k of 157 μmol quanta m^{-2} s^{-1} in the Babin and Morel data set (Fig. 3) and suggests that the Lewis et al. (1985b) mean E_k may have been derived in part from studies in optically shallow mixed layers. Relevant to this point is the fact that Lewis et al.'s (1985b) analysis assumes that photosynthesis extends from the surface to infinite depth. This assumption obviously tends to give as much importance as possible to photosynthesis at low light levels. The combination of this assumption with an E_k value derived from studies in mixed layers of finite optical depth may have biased Lewis et al.'s conclusions (1985b).

Harrison and Platt (1986) subsequently published the results of 700 photosynthesis-irradiance experiments that appear to have provided much of the basis for the mean E_k of 52 W m^{-2} cited by Lewis et al. (1985b). The experiments were conducted in mid-latitudes (41-44°N)

and high latitudes (50-78°N), and histograms of the data have a decidedly log-normal appearance in the former case, i.e., the mean is greater than the median. The median E_k values are 47 and 17 W m^{-2} for the mid- and high-latitude data sets, respectively (Harrison and Platt, 1986, Fig. 3a). The E_k values for samples collected from northern Baffin Bay and from temperate waters off the Scotian Shelf lie between 20 and 30% of the mean surface irradiance (Harrison and Platt, 1986, Fig. 8), i.e., the E_o/E_k ratio is virtually identical to the value of 4 at which Lewis et al. (1985b) conclude that errors in α^* and P_m^* are of equal importance in the calculation of **P***. The Harrison and Platt (1986) data combined with the analysis of Lewis et al. (1985b) do not therefore make a compelling case that **P*** is more sensitive to α^* than P_m^*. The Babin and Morel data (Fig. 3) combined with the analysis presented here indicate that **P*** is more sensitive to P_m^* than α^*.

EFFECTS OF STRATIFICATION AND TEMPORAL VARIABILITY

Chlorophyll concentrations and the characteristics of P* vs. E curves can vary as a function of depth and/or time. Numerous studies have documented the fact that phytoplankton acclimate to changing irradiance (Falkowski and Owens 1980; Sakshaug et al. 1991) and that this acclimation can manifest itself as a systematic variation in P_m^* and α^* with depth in vertically stratified systems (Morel et al. 1996). When the water column is not well mixed, both the chlorophyll concentration and the form and shape of the P* vs. E_o curve may be depth-dependent. If the chlorophyll concentrations are known as a function of depth, they should be included in the least-squares procedure used to estimate E_k and P_m^*. In other words, E_k and P_m^* should be chosen so as to minimize expression 23. In a stratified water column, chlorophyll concentrations will tend to increase with depth to the base of the euphotic zone. The least squares

procedure should weight the P* observations accordingly. Furthermore, E_k will tend to decrease and α^* to increase with increasing depth below the base of the mixed layer. This is true not only because individual species are capable of acclimating to high and low irradiance, but also because systematic variations in the species composition of the phytoplankton community are often observed as a function of depth in stratified systems, with species found deep in the water column best suited to growth in low- light conditions and species near the surface better acclimated to growth in high-light conditions.

This pattern is evident at the oligotrophic site studied by Morel et al. (1996), where E_k (actually K_{PUR}) declined by a factor of ~5 from the surface to the deep chlorophyll maximum and α^* increased by a factor of ~3. One way to resolve this depth dependence is to model E_k and α^* as functions of depth [e.g., the AM model of Morel et al. (1996)]. If E_k and α^* are assumed to be constant, they should be chosen so as to minimize expression 23. Application of a model with constant E_k and α^* to a stratified water column can produce errors in calculated areal photosynthetic rates that are on average no more than those associated with a model incorporating depth-dependent parameters [e.g., Morel et al. (1996), Table 3]. However, the model with constant parameters may do a poor job of reproducing vertical profiles of carbon fixation. Acclimation of phytoplankton to irradiance occurs on a time frame of hours (Falkowski and Raven, 1997). Thus there is certainly reason to expect some change in P* vs. E curve characteristics over the course of 24 hours. This would be true even if irradiance during the photoperiod were constant. It has been known for more than 40 years that many phytoplankton have an endogenous rhythm in their photosynthetic capacity (Doty and Oguri, 1957), and such rhythms have been noted even among phytoplankton growing under conditions of continuous illumination for several months (Rivkin and Putt, 1987). Reports on the magnitude of diurnal

variability are somewhat mixed. Gilstad et al. (1993), for example, found that P_m^* and E_k values varied within 23% of the daily mean in a culture of *Skeletonema costatum* grown on a 12:12 L:D cycle. However, Rivkin and Putt (1987) reported diel variations in the P_m^* of Antarctic phytoplankton that ranged from factors of 1.8 to 15 during the austral summer.

MINIMUM NUMBER OF P-E CURVES REQUIRED FOR ESTIMATES OF PHOTOPERIOD PRODUCTION

Incorporation of vertical and temporal variabilities into models of areal productivity clearly implies that, in general, P* vs. E curves be measured at more than one depth and at more than one time of day. Variations with depth are likely to be monotonic but are typically nonlinear. Characterizing the depth dependence with some degree of statistical confidence (i.e., degrees of freedom) is likely to require measurements from at least 4-5 depths. In the case of temporal variability, it is unlikely that behavior in the afternoon will be a mirror image of behavior during the morning, and a depression of photosynthetic capacity during the midday, especially near the surface, is not uncommon. Given this realization, P* vs. E curves should probably be measured at least five times during the photoperiod, e.g., at sunrise, mid morning, noon, mid afternoon, and sunset. Since such frequent measurements may be impractical on a research cruise, a question more relevant than how many measurements to make during the photoperiod may be, "At what times should the measurements be made?"

In general, measurements made at N points in time can exactly characterize the integral of any function that can be described by a polynomial function of time of order $\leq 2N - 1$. The choice of the times and associated weighting factors for calculating integrals comes under the rubric method of moments and is described by Laws (1997). The simplest form of the method of

moments is Gauss-Legendre Quadrature, and the simplest form of Gauss-Legendre Quadrature is the midpoint rule. The Gauss-Legendre abscissas and weights can be found in Hornbeck (1975) and many other standard references on numerical methods. If the sun rises at 6 a.m. and sets at 6 p.m. and if one samples a function at only one point in time during the photoperiod, then according to Gauss-Legendre Quadrature the best time to sample the function is at noon (midpoint rule). The value of the function at that time will be the average during the photoperiod if the function being integrated can be described by a linear polynomial. If the function is sampled at two times during the photoperiod, the best times to sample are 3.46 hours before and after noon, and the average value of the function is estimated to be the arithmetic mean of the values measured at these two times. The average so calculated will be exact if the function being integrated can be described by a polynomial function of time of order 3 or less. If the function is sampled at three times during the photoperiod, the best times to sample are at midday and 4.65 hours before and after noon. In that case the average value of the function equals 4/9 times the value measured at noon plus 5/18 times the sum of the values measured 4.65 hours before and after noon. The average so calculated will be exact if the function being integrated can be described by a polynomial function of time of order 5 or less.

The time required to incubate and process the samples needed to determine E_k and P_m^* using a photosynthetron imposes a constraint on the number of depths and times at which P* vs. E_o curves can be generated. This problem can be mitigated with the use of variable fluorescence-based methods, which require minimal incubation time.

RELATION OF P* vs. E_o CURVES TO JGOFS CORE MEASUREMENTS OF P VS. Z

If the chlorophyll concentration is independent of depth and irradiance decreases exponentially with depth, then:

$$\begin{aligned}\int_0^D P(z)dz &= chl\int_0^D P^*(z)dz \\ &= \frac{chl}{k}\int_0^{kD} P^*(\zeta/k)d\zeta \\ &= \frac{chl}{k}\int_{E_{os}/E_k e^{-kD}}^{E_{os}/E_k} \frac{P^*(y)}{y}dy\end{aligned} \tag{28}$$

In the second line of equation 28, the dummy variable ζ is the optical depth, and in the third line the dummy variable y is E_o/E_k.

Figure 11 shows the integrands in the second and third lines of (28) and compares these to $P^*(E_o/E_k)$ for mixed layers with optical depths of 2.3, 4.6, and 6.9 (i.e., the base of the mixed layer corresponds to the 10%, 1%, and 0.1% light level, respectively). In each case, E_k was assumed to equal 1/3 of the average irradiance in the mixed layer. The important point about Fig. 11 is that for a given mixed-layer optical depth, the areas under the curves in the first and second columns of Fig. 11 are identical. The areas under the curves in the third column of Fig. 11, however, bear no relationship to the areas under the curves in the first column. This fact underscores why choosing functional expressions and parameter values that give a good description of P* vs. E_o curves does not assure a good description of P* as a function of depth. In other words, there is no well-defined relationship between P* vs. E_o curves and P* vs. z curves. There is, however, a well-defined relationship between the area under the $P^*/(E_o/E_k)$ vs. E_o/E_k curve and the area under the P* vs. kZ curve. The two areas are identical. This equality is the

motivation for choosing analytical functions and parameter values that give a good description of P^*/E_o rather than P^*.

In the more general case, both the chlorophyll concentration and the light attenuation coefficient, k, are functions of depth. In that case the dummy variable $\zeta = kZ$ becomes $\zeta = \int_0^Z k(s)ds$ and

$$\int_0^D P(z)dz = \int_{fE_{os}/E_k}^{E_{os}/E_k} \frac{chl}{ky} P^*(y)dy \qquad (29)$$

where f is the fraction of E_{os} that reaches depth D, i.e., $f = \exp\left(-\int_0^D k(z)dz\right)$. Thus in the general case the analytical function and parameters used to define P* should be chosen to give a good description of $\frac{chl\,P^*}{k\,E_o/E_k}$. Since the chlorophyll concentration will tend to increase and both k and E_o decrease with increasing depth, this goal will give much more emphasis to P* measured at low E_o than would be the case if the analytical function and parameters were chosen so as to give a good fit to P*.

Daily vs. Instantaneous Rates

JGOFS core measurements of P vs. z are based on incubations that last from sunrise to sunset. This is in marked contrast to P* vs. E_o curves, which are based on assays that last no more than 30-60 minutes. Even if the biomass and physiological characteristics of phytoplankton at a given depth were constant throughout the photoperiod, the nonlinear dependence of photosynthetic rate on irradiance would preclude extrapolating short-term P* vs. E_o curves to estimate daily production based on the average irradiance at a given depth. The solution is to

integrate the photosynthetic rate at a given depth over the duration of the photoperiod as discussed above. If the biomass and physiological characteristics of the phytoplankton at a given depth are constant, the daily production at that depth can be calculated by integrating the product of the chlorophyll concentration and $P^*(P_m^*, E_o(t)/E_k))$, where $E_o(t)$ is the time-dependent value of E_o at that depth. In the more general case where the chlorophyll concentration and physiological characteristics of the phytoplankton are changing with time, a numerical integration scheme such as Gauss-Legendre Quadrature can be used to calculate photoperiod production at a fixed depth.

Because of the nonlinear dependence of P* on E_o and the fact that the photosynthetic rate is the product of the chlorophyll concentration and P*, there is no reason to expect that the relationship between production at a given depth and the average chlorophyll concentration and irradiance at that depth should obey the same functional relationship as short-term P* vs. E_o curves (Behrenfeld and Falkowski, 1997a). Nevertheless, models that attempt to relate daily production to chlorophyll concentration and irradiance at a given depth typically adopt the same functional form as short-term P* vs. E_o curves. However, the parameters in the daily production models are given different names to distinguish them from the parameters used to describe short-term P* vs. E_o curves. For example, in the Behrenfeld-Falkowski (1997a) model, P_m^* becomes P_{opt}^* [8] and E_k becomes E_{max}. The choice of analytical function and parameter values to relate the average chlorophyll concentration and irradiance to daily photosynthetic rates becomes a curve-fitting exercise, and as in the analysis of short-term P* vs. E_o curves, it is important to assign the proper weight to observations. If the goal is to obtain good estimates of daily areal production, then the analytical function and parameter values should not be chosen to produce a good fit of

[8] Actually the Behrenfeld-Falkowski symbolism is P_{opt}^B

daily P* to daily irradiance. Instead, the least-squares procedure should be designed to give the best fit to $\frac{\overline{chl}\,\overline{P}^{*}(P^{*}_{opt}, \overline{E}_o / E_{max})}{k\,\overline{E}_o / E_{max}}$, where $\overline{chl}$, $\overline{E}_o$, and $\overline{P}^{*}$ are the chlorophyll concentration, irradiance, and photosynthetic rate per unit chlorophyll averaged over the photoperiod.

Because the curvature of any P* vs. E_o relationship is negative, it follows that the magnitude of the curvature between $\overline{P}^{*}$ and $\overline{E}_o$ will be less than the magnitude of the curvature between P* and E_o. This fact is illustrated in Fig. 12, which shows $P^*(E_o/E_k)$ and $P^*(\overline{E}_o/E_k)$ for the simple case where $P^*(E_o/E_k) = \tanh(E_o/E_k)$ and E_o was assumed to be a linear function of time from sunrise to midday. Although the initial slopes and asymptotic values of the two functions are identical, $P^*(\overline{E}_o/E_{max}) < P^*(E_o/E_k)$ for all intermediate values of the arguments.

Because the temporal dependence of E_o during the photoperiod will, in general, be nonlinear and because the integrated forms of equations 4-8 bear no simple relationship to the integrands, it may be desirable for curve-fitting purposes to adopt more flexible functions than equations 4-8. A general exponential representation of P* vs. $\overline{E}_o$ curves in the absence of photoinhibition takes the form

$$P^{*} = P^{*}_{opt}\left(\frac{e^{(\varepsilon+1)\overline{E}_o / E_{max}} - 1}{e^{(\varepsilon+1)\overline{E}_o / E_{max}} + \varepsilon}\right) \tag{30}$$

where $\varepsilon \geq -1$ (Chisholm, 2000). Values of ε equal to -1, 0, and 1 correspond to equations 4, 5, and 7, respectively.

RELATION OF CORE PROFILES AND P VS. E_o CURVES TO SATELLITE MAPS OF OCEAN COLOR AND ESTIMATES OF BASIN SCALE PRIMARY PRODUCTION

Extending models of daily primary production with the use of data derived from satellites to estimate annual primary production on a basin or global scale requires characterizing the parameters in P* vs. $\overline{E}_o$ in terms of parameters that can be estimated from satellites. A thorough discussion of these issues is found in Behrenfeld and Falkowski (1997a,b). As noted by Behrenfeld and Falkowski (1997b), most of the discrepancies between estimates of annual primary production based on these models can be traced to differences in input chlorophyll fields. The highest estimates have been based on an algorithm (Sathyendranath and Platt, 1989) that produced CZCS-based surface chlorophyll concentrations on average 100% higher than values produced by a standard NASA algorithm when the two were compared over the North Atlantic basin.

With respect to P*, most models differ primarily in their estimation of P^*_{opt} and the functional form of $f(\overline{E}_o/E_{max})$. Virtually all models assume that one or another of equations 4-8 describes the relationship between $\overline{E}_o$ and P*. Strictly speaking, this makes no sense if one or another of equations 4-8 describes the instantaneous relationship between E_o and P*, since as noted above $f(\overline{E}_o/E_{max}) < f(E_o/E_k)$ for all irradiances between zero and infinity. Similar descriptions of field data can often be obtained with the right combination of analytical model and parameter values. This fact probably accounts for the similarity of basin and global scale production estimates when the calculations are based on the same chlorophyll fields (Behrenfeld and Falkowski, 1997b).

Perhaps the most important point relative to the choice of model and parameter values is to choose a least-square scheme that minimizes an expression that can be directly related to the

integral of interest. In general selecting a model and parameter values that give a good fit to P* vs. E_o or P* vs. $\overline{E}_o$ is a poor way to select a model and parameter values if one is interested in estimating areal photosynthetic rates. As explained above, the best least-squares scheme will seek to give a good description of $\frac{chl P^*}{k E_o}$ or $\frac{\overline{chl}\,\overline{P}^*}{k \overline{E}_o}$. Estimating $\overline{P}^*$ requires numerically integrating the results of short-term P* vs. E_o experiments. This is best done when the sampling times are chosen to facilitate use of the most efficient numerical integration techniques.

ACKNOWLEDGEMENTS

This manuscript benefited from the constructive comments of Shubha Sathyendranath. This work was supported by a generous grant from the International Joint Global Ocean Flux Study and from the United States JGOFS Synthesis and Modeling Program (OCE-97-25966).

Table 1. Ratio of oxygen-based gross production to ^{14}C-based photosynthesis $\left(\frac{\text{moles O}_2}{\text{moles CO}_2}\right)$

$\frac{\text{gross oxygen}}{^{14}\text{C photosynthesis}}$	Duration of incubation (h)	Location of study	Reference
2.2 ± 0.5	4	Bedford Basin	Grande et al. (1991)
1.5 ± 0.3	4	*Synechococcus* culture	Grande et al. (1991)
2.0	24	Estuary – Southampton Water	Williams et al. (1979)
2.4	24	North Atlantic bloom	Bender et al. (1992)
2.5	24	Arabian Sea	Laws et al. (2000)
2.2	24	Equatorial Sea	Bender et al. (1999)
1.2-1.6	12	N. Pacific subtropical gyre	Grande et al. (1989)
1.6-2.0	24	MERL tanks	Bender et al. (1987)
1.3-2.1	12	MERL tanks	Bender et al. (1987)

Table 2. Ratio of ^{18}O-based gross photosynthesis to gross photosynthesis estimated from light-and-dark bottle incubations.

Ratio	Reference
1.1-1.4	Bender et al. (1987)
0.8-1.1	Grande et al. (1989)
0.75-2.1	Grande et al. (1991)

REFERENCES

Allali, K., A. Bricaud, M. Babin, A. Morel, and P. Chang. 1995. A new method for measuring spectral absorption coefficients of marine particles. Limnol. Oceanogr. 40: 1526-1532.

Allen, C. B., J. Kanda, and E. A. Laws. 1996. New production and photosynthetic rates within and outside a cyclonic mesoscale eddy in the North Pacific subtropical gyre. Deep-Sea Res. 43: 917-936.

Babin, M., A. Morel, H. Claustre, A. Bricaud, Z. Kolber, and P. G. Falkowski. 1996. Nitrogen- and irradiance-dependent variations of the maximum quantum yield of carbon fixation in eutrophic, mesotrophic and oligotrophic marine systems. Deep-Sea Res. 43: 1241-1272.

Babin, M., A. Morel, and R. Gagnon. 1994. An incubator designed for extensive and sensitive measurements of phytoplankton photosynthetic parameters. Limnol. Oceanogr. 39: 694-702.

Baker, K. S., and R. C. Smith. 1982. Bio-optical classification and model of natural waters, 2. Limnol. Oceanogr. 27: 7555-7570.

Behrenfeld, M. J., and P. G. Falkowski. 1997a. Photosynthetic rates derived from satellite-based chlorophyll concentration. Limnol. Oceanogr. 42: 1-20.

Behrenfeld, M. J. and P. G. Falkowski. 1997b. A consumer's guide to phytoplankton primary productivity models. Limnol. Oceanogr. 42: 1479-1491.

Bender, M. L., H. Ducklow, J. Kiddon, J. Marra, and J. Martin. 1992. The carbon balance during the 1989 spring bloom in the North Atlantic Ocean, 47°N, 20°W. Deep-Sea Res. 39: 1707-1725.

Bender, M. L., K. Grande, K. Johnson, J. Marra, P. J. leB. Williams, J. Sieburth, M. Pilson, C. Langdon, G. Hitchcock, J. Orchardo, C. Hunt, P. Donaghay, and K. Heinemann. 1987. A comparison of four methods for determining planktonic community production. Limnol. Oceanogr. 32: 1085-1098.

Bender, M. L., J. Orchardo, M.-L. Dickson, R. Barber, and S. Lindley. 1999. In vitro O2 fluxes compared with ^{14}C production and other rate terms during the JGOFS Equatorial Pacific experiment. Deep-Sea Res. 46: 637-654.

Berner, T., A. Dubinsky, K. Wyman, and P. G. Falkowski. 1989. Photoadaptation and the "package" effect in *Dunaliella tertiolecta* (Chlorophyceae). J. Phycol. 25: 70-78.

Buechel, C., and C. Wilhelm. 1993. In vivo analysis of slow chlorophyll fluorescence induction kinetics in algae: Progress, problems and perspectives. Photochem. Photobiol. 58: 137-148.

Bidigare, R. R., M. E. Ondrusek, J. H. Morrow, and D. A. Kiefer. 1990a. In vivo absorption properties of algal pigments. Ocean Opt. 1302: 290-302.

Bidigare, R. R., O. Schofield, and B. B. Prézelin. 1990b. Influence of zeaxanthin on quantum yield of photosynthesis of *Synechococcus* clone WH7803 (DC2) Mar. Ecol. Prog. Ser. 56: 177-188.

Blackburn, N., T. Fenchel, and J. Mitchell. 1998. Microscale nutrient patches in planktonic habitats shown by chemotactic bacteria. Science 282: 2254-2256.

Bricaud, A., A. Morel, and L. Prieur. 1983. Optical efficiency factors of some phytoplankters. Limnol. Oceanogr. 28: 816-832.

Carpenter, E. J., and J. S. Lively. 1980. Review of estimates of algal growth using ^{14}C tracer technique. Brookhaven Symp. Biol. 31: 161-178. Plenum.

Cassie, M. 1959a. An experimental study of factors inducing aggregation in marine plankton. New Zealand J. Sci. 2: 339-365.

Cassie, M. 1959b. Micro-distribution of plankton. New Zealand J. Sci. 2: 398-409.

Chisholm, J. R. M. 2000. Calcification by crustose coralline algae on the northern Great Barrier Reef, Australia. Limnol. Oceanogr. 45: 1476-1484.

Cleveland, J. S., M. J. Perry, D. A. Kiefer, and M. C. Talbot. 1989. Maximal quantum yield of photosynthesis in the Northwestern Sargasso Sea. J. Mar. Res. 47: 869-886.

Cleveland, J. S., and A. D. Weidemann. 1993. Quantifying absorption by aquatic particles: a multiple scattering correction for glass-fiber filters. Limnol. Oceanogr. 38: 1321-1327.

Cottrell, M. T., and C. A. Suttle. 1995. Dynamics of a lytic virus infecting the photosynthetic marine picoflagellate *Micromonas pusilla*. Limnol. Oceanogr. 40: 730-739.

Davis, C. S., S. M. Gallager, and A. R. Solow. 1992. Microaggregations of oceanic plankton observed by towed video microscopy. Science 257: 230-232.

DiTullio, G. R., and E. A. Laws. 1986. Diel periodicity of nitrogen and carbon assimilation in five species of marine phytoplankton: accuracy of methodology for predicting N-assimilation rates and N/C composition ratios. Mar. Ecol. Prog. Ser. 32: 123-132.

Doty, M. S. and M. Oguri. 1957. Evidence for a photosynthetic daily periodicity. Limnol. Oceanogr. 2: 37-40.

Doucha, J., and S. Kubin. 1976. Measurement of in vivo absorption spectra of microscopic algae using bleached cells as a reference sample. Arch. Hydrobiol. 49 (suppl.): 199-213.

Dring, M. J., and D. H. Jewson. 1982. What does ^{14}C uptake by phytoplankton really measure? A theoretical modeling approach. Proc. R. Soc. Lond. B 214: 351-368.

Duysens, L. M. N. 1956. The flattening of the absorption spectra of suspensions as compared to that of solutions. Biochem. Biophys. Acta 19: 1-12.

Escoubas, J.-M, M. Lomas, J. LaRoche, and P. G. Falkowski. 1995. Light intensity regulation of *cab* gene transcription is signaled by the redox state of the plastoquinone pool. Proc. Natl. Acad. Sci. USA 92: 10237-10241.

Emerson, R., and W. Arnold. 1932. The photochemical reaction in photosynthesis. J. Gen. Physiol. 16: 191-205.

Falkowski, P. G. 1980. Light-shade adaptation in marine phytoplankton. pp. 99-119 in Falkowski, P. G. (ed.), *Primary Productivity in the Sea*, Plenum Publishing Corp., New York.

Falkowski, P. G. 1981. Light-shade adaptation and assimilation numbers. J. Plank. Res. 3: 203-216.

Falkowski, P. G. 1992. Molecular ecology of phytoplankton photosynthesis. pp. 47-67 in Falkowski, P. G. and A. Woodhead (eds.), *Primary Productivity and Biogeochemical Cycles in the Sea*. Plenum Press, New York and London.

Falkowski, P. G., and D. A. Kiefer. 1985. Chlorophyll *a* fluorescence in phytoplankton: relationship to photosynthesis and biomass. J. Plank. Res. 7: 715-731.

Falkowski, P. G., and Z. Kolber. 1993. Estimation of phytoplankton photosynthesis by active fluorescence. In W. K. Li and S. Y. Maestrini (eds.), *Measurement of Primary Production from the Molecular to the Global Scale*. Proceedings of a symposium held in La Rochelle, 21-24 April 1992. Pp. 92-103,

Falkowski, P. G., and Z. Kolber. 1995. Variations in chlorophyll fluorescence yields in phytoplankton in the world oceans. Aust. J. Plant. Physiol. 22: 341-355.

Falkowski, P. G. and T. G. Owens. 1980. Light-shade adaptation: Two strategies in marine phytoplankton. Plant Physiol. 66: 592-595.

Falkowski, P. G. and J. A. Raven. 1997. Aquatic Photosynthesis. Blackwell Science, London.

Field, C. B., M. J. Behrenfeld, J. T. Randerson, and P. Falkowski. 1998. Primary production of the biosphere: Integrating terrestrial and oceanic components. Science 281: 237-240.

Fitzwater, S. E., G. A. Knauer, and J. H. Martin. 1982. Metal contamination and its effect on primary production measurements. Limnol. Oceanogr. 27: 544-552.

Frenette, J-J., S. Demers, L. Legendre, and J. Dodson. 1993. Lack of agreement among models for estimating the photosynthetic parameters. Limnol. Oceanogr. 38: 679-687.

Gaffron, H., and K. Wohl. 1936. The theory of assimilation. I and II. Naturwissenschaften 24: 81-90, 103-107.

Gaxiola-Castro, G., S. Alvarez-Borrego, M. F. Lavin, A. Zirino, and S. Najera-Martinez. 1999. Spatial variability of the photosynthetic parameters and biomass of the Gulf of California phytoplankton. J. Plank. Res. 21: 231-245.

Geider, R. J., H. L. MacIntyre, and T. M. Kana. 1998. A dynamic regulatory model of phytoplanktonic acclimation to light, nutrients, and temperature. Limnol. Oceanogr. 43: 679-694.

Geider, R. J., and B. A. Osborne. 1987. Light absorption by a marine diatom: Experimental observations and theoretical calculations of the package effect in a small Thalassiosira species. Mar. Biol. 96: 299-308.

Gieskes, W. W. C., G. W. Kraay, and M. A. Baars. 1979. Current ^{14}C methods for measuring primary production: Gross underestimates in oceanic waters. Neth. J. Sea Res. 13: 58-78.

Gilstad, M., G. Johnsen and E. Sakshaug. 1993. Photosynthetic parameters, pigment composition and respiration rates of the marine diatom *Skeletonema costatum* grown in continuous light and a 12:12 h light-dark cycle. J. Plank. Res. 15: 939-951.

Grande, K. D., M. L. Bender, B. Irwin, and T. Platt. 1991. A comparison of net and gross rates of oxygen production as a function of light intensity in some natural plankton populations and in a *Synechococcus* culture. J. Plank. Res. 13: 1-16.

Grande, K., P. Kroopnick, D. Burns, and M. L. Bender. 1982. ^{18}O as a tracer for measuring gross primary productivity in bottle experiments. [Abstr.] Eos 63: 107.

Grande, K. D., P. J. leB. Williams, J. Marra, D. A. Purdie, K. Heinemann, R. W. Eppley, and M. L. Bender. 1989. Primary production in the North Pacific gyre: a comparison of rates determined by the ^{14}C, O_2 concentration and ^{18}O methods. Deep-Sea Res. 36: 1621-1634.

Greene, R. M., Z. S. Kolber, D. G. Swift, N. W. Tindale, and P. G. Falkowski. 1994. Physiological limitation of phytoplankton photosynthesis in the eastern equatorial Pacific determined from variability in the quantum yield of fluorescence. Limnol. Oceanogr. 39: 1061-1074.

Harrison, W. G., and T. Platt. 1980. Variations in assimilation number of coastal marine phytoplankton: effects of environmental co-variates. J. Plank. Res. 2: 249-260.

Harrison, W. G., and T. Platt. 1986. Photosynthesis-Irradiance relationships in polar and temperate phytoplankton populations. Polar Biol. 5: 153-164.

Hartig, P., K. Wolfstein, S. Lippemeier, and F. Colijn. 1998. Photosynthetic activity of natural microphytobenthos populations measured by fluorescence (PAM) and ^{14}C-tracer methods: a comparison. Mar. Ecol. Prog. Ser. 166: 53-62.

Hatchard, C. G., and C. A. Parker. 1956. A new sensitive chemical actinometer II. Potassium ferrioxalate as a standard chemical actinometer. Proc. R. Soc. Lond. A 235: 518-536.

Herbland, A., A. LeBoutellier, and P. Raimbault. 1985. Size structure of phytoplankton biomass in the equatorial Atlantic Ocean. Deep-Sea Res. 32: 819-836.

Hewes, C. D., and O. Holm-Hansen. 1983. A method for recovering nanoplankton from filters for identification with the microscope: The filter-transfer-freeze (FTF) technique. Limnol. Oceanogr. 28: 389-394.

Higgins, H. W., and D. J. Mackey. 2000. Algal class abundances, estimated from chlorophyll and carotenoid pigments, in the western Equatorial Pacific under El Niño and non-El Niño conditions. Deep-Sea Res. 47: 1461-1483.

Hoepffner, N. and S. Sathyendranath. 1991. Effect of pigment composition on absorption properties of phytoplankton. Mar. Ecol. Prog. Ser. 73: 11-23.

Hornbeck, R. W. 1975. *Numerical Methods*. Quantum Publishers. New York. 310 pp.

Jassby, A. D., and T. Platt. 1976. Mathematical formulation of the relationship between photosynthesis and light for phytoplankton. Limnol. Oceanogr. 21: 540-547.

Jerlov, N. G. 1968. *Optical Oceanography*. Elsevier. 194 pp.

Johnsen, G., N. B. Nelson, R. V. M. Jovine, and B. B. Prézelin. 1994. Chromoprotein- and pigment-dependent modeling of spectral light absorption in two dinoflagellates, *Prorocentrum minimum* and *Heterocapsa pygmaea*. Mar. Ecol. Prog. Ser. 114: 245-258.

Johnsen, G., and E. Sakshaug. 1993. Bio-optical characteristics and photoadaptive responses in the toxic and bloom-forming dinoflagellates *Gyrodinium aureolum*, *Gymnodinium galatheanum*, and two strains of *Prorocentrum minimum*. J. Phycol. 29: 627-642.

Karl, D. M., D. V. Hebel, K. Björkman, and R. M. Letelier. 1998. The role of dissolved organic matter release in the productivity of the oligotrophic North Pacific Ocean. Limnol. Oceanogr. 43: 1270-1286.

Kiefer, D. A., and J. D. H. Strickland. 1970. A comparative study of photosynthesis in seawater samples incubated under two types of light attenuator. Limnol. Oceanogr. 15: 408-412.

Kierstead, H., and L. B. Slobodkin. 1953. The size of water masses containing plankton blooms. J. Mar. Res. 12: 141-155.

Kirk, J. T. O. 1975. A theoretical analysis of the contribution of algal cells to the attenuation of light within natural waters. I. General treatment of pigmented cells. New Phytologist 75: 11-20.

Kishino, M., M. Takahashi, N. Okami, and S. Ichimura. 1985. Estimation of the spectral absorption coefficients of phytoplankton in the sea. Bull. Mar. Sci. 37: 634-642.

Koblentz-Mishke, O. J., V. V. Volkovinsky, J. G. Kabanova. 1970. in *Scientific Exploration of the South Pacific*, W. S. Wooster (Ed.), National Academy of Science, Washington, D.C. pp. 183-193.

Kok, B. 1948. A critical consideration of the quantum yield of *Chlorella*-photosynthesis. Enzymologia 13: 1-56.

Kolber, Z., and P. G. Falkowski. 1993. Use of active fluorescence to estimate phytoplankton photosynthesis in situ. Limnol. Oceanogr. 38: 1646-1665.

Kolber, Z., J. Zehr, and P. G. Falkowski. 1988. Effects of growth irradiance and nitrogen limitation on photosynthetic energy conversion in Photosystem II. Plant Physiol. 88: 923-929.

Konovalov, B. V., and O. D. Bekasova. 1969. Method of determining the pigment content of marine phytoplankton without extraction. Oceanology 9: 717-725.

Langdon, C. 1988. On the causes of interspecific differences in the growth-irradiance relationship for phytoplankton. II. A general review. J. Plank. Res. 10: 1291-1312.

Laws, E. A. 1984. Improved estimates of phytoplankton carbon based on ^{14}C incorporation into chlorophyll *a*. J. Theor. Biol. 110: 425-434.

Laws, E.A. 1991. Photosynthetic quotients, new production, and net community production in the open ocean. Deep-Sea Res. 38: 143-167.

Laws, E. A. 1997. Mathematical Methods for Oceanographers: An Introduction. Wiley-Interscience, New York.

Laws, E.A., and T.T. Bannister. 1980. Nutrient and light-limited growth of *Thalassiosira fluviatilis* in continuous culture, with implications for phytoplankton growth in the ocean. Limnol. and Oceanogr. 25: 457-473.

Laws, E.A., G.R. DiTullio, P.R. Betzer, and S. Hawes. 1990. Primary production in the deep blue sea. Deep-Sea Res. 37: 715-730.

Laws, E.A., G.R. DiTullio, and D.G. Redalje. 1987. High phytoplankton growth and production rates in the North Pacific subtropical gyre. Limnol. and Oceanogr. 32: 905-918.

Laws, E. A., M. R. Landry, R. T. Barber, L. Campbell, M.-L. Dickson, and J. Marra. 2000. Carbon cycling in primary production bottle incubations: inferences from grazing experiments and photosynthetic studies using ^{14}C and ^{18}O in the Arabian Sea. Deep-Sea Res. II 47: 1339-1352.

Lee, Z. P., K. L. Carder, J. Marra, R. G. Steward, and M. J. Perry. 1996. Estimating primary production at depth from remote sensing. Appl. Optics 35: 463-474.

Legendre, L., S. Demers, C. M. Yentsch, and C. S. Yentsch. 1983. The ^{14}C method: Patterns of dark CO_2 fixation and DCMU correction to replace the dark bottle. Limnol. Oceanogr. 28: 996-1003.

Leighton, W. G. and G. S. Forbes. 1930. Precision actinometry with uranyl oxalate. J. Amer. Chem. Soc. 52: 3139-3152.

Letelier, R. M., J. E. Dore, C. D. Winn, and D. M. Karl. 1996. Seasonal and interannual variations in photosynthetic carbon assimilation at Station ALOHA. Deep-Sea Res. II(Part 2, Topical Studies in Oceanography) 43: 467-490.

Lewis, M. R., and J. C. Smith. 1983. A small volume, short-incubation time method for measurement of photosynthesis as a function of incident irradiance. Mar. Ecol. Prog. Ser. 13: 99-102.

Lewis, M. R., O. Ulloa, and T. Platt. 1988. Photosynthetic action, absorption and quantum yield spectra for a natural population of *Oscillatoria* in the North Atlantic. Limnol. Oceanogr. 33: 92-99.

Lewis. M. R., R. E. Warnock, B. Irwin, and T. Platt. 1985a. Measuring photosynthetic action spectra of natural phytoplankton populations. J. Phycol. 21: 310-315.

Lewis. M. R., R. E. Warnock and T. Platt. 1985b. Absorption and photosynthetic action spectra for natural phytoplankton populations: Implications for production in the open ocean. Limnol. Oceanogr. 30: 794-806.

Ley, A. C., and D. Mauzerall. 1982. Absolute absorption cross-sections for Photosystem II and the minimum quantum requirement for photosynthesis in *Chlorella vulgaris*. Biochim. Biophys. Acta 680: 95-106.

Li, W. K. W. 1987. Experimental approaches to field measurements: Methods and interpretation. In: Photosynthetic picoplankton, T. Platt and W. K. W. Li (eds), Canadian Bulletin of Fisheries and Aquatic Science 214: 251-286.

Li, W. K. W., D. V. Subba Rao, W. G. Harrison, J. C. Smith, J. J. Cullen, B. Irwin, and T. Platt. 1983. Autotrophic picoplankton in the tropical ocean. Science 219: 292-295.

Lindeman, R. L. 1942. The trophic-dynamic aspect of ecology. Ecology 23: 399-418.

Lohrenz, S. E., Wisenburg, D. A., C. R. Rein, R. A. Arnone, C. D. Taylor, G. A. Knauer, and A. H. Knap. 1992. A comparison of in situ and simulated in situ methods for estimating primary production. J. Plank. Res. 14: 201-221.

Longhurst, A., S. Sathyendranath, T. Platt, and C. Caverhill. 1995. An estimate of global primary production in the ocean from satellite radiometer data. J. Plank. Res. 17: 1245-1271.

Marra, J. and K. R. Heinemann. 1984. A comparison between noncontaminating and conventional incubation procedures in primary production measurements. Limnol. Oceanogr. 29: 389-392.

Marra, J. and K. R. Heinemann. 1987. Primary production in the North Pacific Central Gyre: some new measurements based on ^{14}C. Deep-Sea Res. 34: 1821-1829.

Maske, H., and E. Garcia-Mendoza. 1994. Adsorption of dissolved organic matter to the inorganic filter substrate and its implications for ^{14}C uptake measurements. Appl. Environ. Microbiol. 60: 3887-3889.

Mitchell, B. G. 1990. Algorithms for determining the absorption coefficient of aquatic particulates using the quantitative filter technique (QFT). Ocean Opt. 1302: 137-148.

Mitchell, B. G., and D. A. Kiefer. 1988. Variability in pigment specific particulate fluorescence and absorption spectra in the northeastern Pacific Ocean. Deep-Sea Res. 35: 665-689.

Moore, L. R., R. Goericke, and S. W. Chisholm. 1995. Comparative physiology of *Synechococcus* and *Prochlorococcus*: influence of light and temperature on growth, pigments, fluorescence and absorption properties. Mar. Ecol. Prog. Ser. 116: 259-275.

Morel, A. 1978. Available, usable and stored radiant energy in relation to marine photosynthesis. Deep-Sea Res. 25: 673-688.

Morel, A. 1988. Optical modeling in the upper ocean in relation to its biogenous matter content (Case I waters). J. Geophys. Res. 93: 263-306.

Morel, A., and J. M. André. 1991. Pigment distribution and primary production in the Western Mediterranean as derived and modeled from Coastal Color Zone Scanner observations. J. Geophys. Res. 96: 12,685-12,698.

Morel, A., and D. Antoine. 1994. Heating rate within the upper ocean in relation to its bio-optical state. J. Geophys. Res. 24: 1652-1665.

Morel, A., D. Antoine, M. Babin and Y. Dandonneau. 1996. Measured and modeled primary production in the northeast Atlantic (EUMELI JGOFS program): The impact of natural variations in photosynthetic parameters on model predictive skill. Deep-Sea Res. 43: 1273-1304.

Morel, A. and A. Bricaud. 1981. Theoretical results concerning light absorption in a discrete medium, and application to specific absorption of phytoplankton. Deep-Sea Res. 11: 1375-1393.

Morel, A., L. Lazzara, and J. Gostan. 1987. Growth rate and quantum yield time response for a diatom to changing irradiances (energy and color). Limnol. Oceanogr. 32: 1066-1084.

Morris, I., C. M. Yentsch, and C. S. Yentsch. 1971. Relationship between light CO_2 fixation and dark CO_2 fixation by marine algae. Limnol. Oceanogr. 26: 854-858.

Myers, J. H. 1980. On the algae: Thoughts about physiology and measurements of efficiency. In Falkowski, P. G. (ed.), *Primary Productivity in the Sea*. Plenum Press, New York, pp. 1-16.

Nelson, N. B., B. B. Prézelin, and R. R. Bidigare. 1993. Phytoplankton light absorption and the package effect in California coastal waters. Mar. Ecol. Prog. Ser. 94: 217-227.

Palmisano, A. C., and J. B. SooHoo. 1985. Photosynthesis-irradiance relationships in sea ice microalgae from McMurdo Sound, Antarctica. J. Phycol. 21: 341-346.

Peterson, B. J. 1980. Aquatic primary productivity and the ^{14}C-CO_2 method: A history of the productivity problem. Ann. Rev. Ecol. Syst. 11: 359-385.

Platt, T. 1972. Local phytoplankton abundance and turbulence. Deep-Sea Res. 19: 183-187.

Platt, T., C. I. Gallegos, and W. G. Harrison. 1980. Photoinhibition of photosynthesis in natural assemblages of marine phytoplankton. J. Mar. Res. 38: 687-701.

Platt, T., W. G. Harrison, B. Irwin, E. P. Horne, and C. L. Gallegos. 1982. Photosynthesis and photoadaptation of marine phytoplankton in the Arctic. Deep-Sea Res. 29: 1159-1170.

Platt, T., and S. Sathyendranath. 1988. Oceanic primary production: Estimation by remote sensing at local and regional scales. Science 241: 1613-1620.

Platt, T., and S. Sathyendranath. 1993. Estimators of primary production for interpretation of remotely sensed data on ocean color. J. Geophys. Res. 98: 14,561-14,576

Prasil, O., Z. Kolber, J. A. Berry, and P. G. Falkowski. 1996. Cyclic electron flow around Photosystem II in vivo. Photosynthesis Res. 48: 395-410.

Raven, J. A. 1984a. *Energetics and transport in aquatic plants*. New York. AR Liss.

Raven, J. A. 1984b. A cost-benefit analysis of photon absorption by photosynthetic unicells. New Phytol. 94: 593-625.

Raven, J. A. 1993. Carbon: A phycocentric view. pp. 123-152 in Evans, G. T., and M. J. R. Fasham (eds.), *Towards a Model of Ocean Biogeochemical Processes*. Springer-Verlag, Berlin.

Raven, J. A., and J. Beardall. 1981. Respiration and photorespiration. Fisheries and Aquat. Sci. 210: 55-82.

Reed, R. K. 1977. On estimating insolation over the ocean. J. Phys. Oceanogr. 7: 482-485.

Renk, H. and S. Ochocki. 1998. Photosynthetic rate and light curves of phytoplankton in the southern Baltic. Oceanologia 40: 331-344.

Renk, H., S. Ochocki, H. Chmielowski, S. Gromisz, J. Nakonieczny, M. Pastuszak, and M. Zalewski. 1999. Photosynthetic light curves in the Pomeranian Bay (Baltic Sea). Oceanologia 41: 355-371.

Rivkin, R. B. and M. Putt. 1987. Diel periodicity of photosynthesis in polar phytoplankton: Influence on primary production. Science 238: 1285-1288.

Roy, S., R. P. Harris, and S. Poulet. 1989. Inefficient feeding by *Calanus helgolandicus* and *Temora longicornis* on *Coscinodiscus wailesii*: estimation using chlorophyll-type pigments and effects on dissolved free amino acids. Mar. Ecol. Prog. Ser. 52: 145-153.

Ryther, J. H. 1956. Interrelation between photosynthesis and respiration in the marine flagellate, *Dunaliella euchlora*. Nature 178: 861-862.

Saijo, Y., and K. Takesue. 1965. Further studies on the size distribution of photosynthesizing phytoplankton in the Indian Ocean. J. Oceanogr. Soc. Japan 20: 10-17.

Sakshaug, E., A. Bricaud, Y. Dandonneau, P. G. Falkowski, D. A. Kiefer, L. Legendre, A. Morel, J. Parslow, and M. Takahashi. 1997. Parameters of photosynthesis: Definitions, theory and interpretations of results. J. Plank. Res. 19: 1637-1760.

Sakshaug, E., G. Johnsen, K. Andresen and M. Vernet. 1991. Modeling of light-dependent algal photosynthesis and growth: experiments with the Barents Sea diatoms *Thalassiosira nordenskioeldii* and *Chaetoceros furcellatus*. Deep-Sea Res. 38: 415-430.

Sathyendranath, S., and T. Platt. 1989. Remote sensing of ocean chlorophyll: Consequence of non-uniform pigment profile. Appl. Opt. 28: 490-495.

Sathyendranath, S., T. Platt, C. M. Caverhill, R. E. Warnock, and M. R. Lewis. 1989. Remote sensing of oceanic production: Computations using a spectral model. Deep-Sea Res. 36: 431-453.

Sathyendranath, S., T. Platt, V. Stuart, B. D. Irwin, M. J. W. Veldhuis, G. W. Kraay, and W. G. Harrison. 1996. Some bio-optical characteristics of phytoplankton in the NW Indian Ocean. Mar. Ecol. Prog. Ser. 132: 299-311.

Sathyendranath, S., V. Stuart, B. D. Irwin, H. Maass, G. Savidge, L. Gilpin, and T. Platt. 1999. Seasonal variations in bio-optical properties of phytoplankton in the Arabian Sea. Deep-Sea Res. 46: 633-653.

Schofield, O., B. B. Prézelin, R. R. Bidigare, and R. C. Smith. 1993. In situ photosynthetic quantum yield. Correspondence to hydrographic and optical variability within the Southern California Bight. Mar. Ecol. Prog. Ser. 93: 25-37.

Seliger, H. H., and W. McElroy. 1965. *Light: Physical and Biological Action*. Academic Press, New York. 419 pp.

Sheldon, R. W., W. H. Sutcliffe, and A. Prakash. 1973. The production of particles in the surface waters of the ocean with particular reference to the Sargasso Sea. Limnol. Oceanogr. 18: 719-733.

Shuter, B., A. 1979. A model of physiological adaptation in unicellular algae, J. Theor. Biol. 78: 519-552.

Siefermann-Harms, D. 1985. Carotenoids in photosynthesis. I. Location in photosynthetic membranes and light-harvesting function. Biochim. Biophys. Acta 811: 325-355.

Silver, M. W., A. L. Shanks, and J. D. Trent. 1978. Marine snow: Microplankton habitat and source of small-scale patchiness in pelagic populations. Science 201: 371-373.

Sosik, H., and B. G. Mitchell. 1995. Light absorption by phytoplankton, photosynthetic pigments and detritus in the California Current system. Deep-Sea Res. 42: 1717-1748.

Steemann-Nielsen, E. 1952. The use of radioactive carbon (^{14}C) for measuring organic production in the sea. J. Cons. Perm. Int. Explor. Mer 18: 117-140.

Steemann-Nielsen, E. 1955. The interaction of photosynthesis and respiration and its importance for the determination of ^{14}C discrimination in photosynthesis. Physiol. Plant. 8: 945-953.

Stramski, D., A. Shalapyonok, and R. A. Reynolds. 1995. Optical characterization of the unicellular cyanobacterium *Synechococcus* grown under a day-night cycle in natural irradiance. J. Geophys. Res. 100: 13,295-13,307.

Strickland, J. D. H. 1958. Solar radiation penetrating the ocean. A review of requirements, data and methods of measurement, with particular reference to photosynthetic productivity. J. Fish. Res. Bd. Canada 15: 453-493.

Suggett, D., G. Kraay, P. Holligan, M. Davey, J. Aiken, and R. Geider. 2001. Assessment of photosynthesis in a spring cyanobacterial bloom by use of a fast repetition rate fluorometer. Limnol. Oceanogr. 46: 802-810.

Taguchi, S. 1983. Dark fixation of CO_2 in the subtropical north Pacific Ocean and the Weddell Sea. Bull Plank. Soc. Japan 30: 115-124.

Taguchi, S., G. R. DiTullio, and E. A. Laws. 1988. Physiological characteristics and production of mixed layer and chlorophyll maximum phytoplankton populations in the Caribbean Sea and western Atlantic Ocean. Deep-Sea Res. 35: 1363-1377.

Tassan, S., and G. M. Ferrari. 1995. An alternative approach to absorption measurements of aquatic particles retained on filters. Limnol. Oceanogr. 40: 1358-1368.

Trüper, H. and C. S. Yentsch. 1967. Use of glass fiber filters for the rapid preparation of *in vivo* absorption spectra of photosynthetic bacteria. J. Bacteriol. 94: 1255-1256.

Tyler, J. E. (ed.) 1966. *Report on the second meeting of the Joint Group of Experts on Photosynthetic Radiant Energy*. UNESCO Tech. Paper Mar. Sci. 2: 1-11.

Vassiliev, I. R., Z. Kolber, K. D. Wyman, D. Mauzerall, V. Shukla, and P. G. Falkowski. 1995. Effects of iron limitation on Photosystem II composition and light utilization in *Dunaliella tertiolecta*. Plant Physiol. 109: 963-972.

Vedernikov, V. I. 1982. Assimilation number and its variations in cultures and natural populations of marine planktonic algae. Oceanic Phytoplank. Primary Prod. 114: 92-112.

Venrick, E. L. 1971. The statistics of subsampling. Limnol. Oceanogr. 16: 811-818.

Venrick, E. L., J. R. Beers, and J. F. Heinbokel. 1977. Possible consequences for containing microplankton for physiological rate measurements. J. Exp. Mar. Biol. Ecol. 26: 55-76.

Venrick, E. L., J. A. McGowan, and A. W. Mantyla. 1973. Deep maxima of photosynthetic chlorophyll in the Pacific Ocean. Fish. Bull. 71: 41-42.

Verduin, J. 1960. Phytoplankton communities of western Lake Erie and the CO_2 and O_2 changes associated with them. Limnol. Oceanogr. 5: 372-380.

von Boekel, W. H. M., F. C. Hanse, R. Riegman, and R. P. M. Bak. 1992. Lysis-induced decline of a Phaeocystis bloom and coupling with the microbial food-web. Mar. Ecol. Prog. Ser. 81: 269-276.

Weger, H. G., R. Herzig, P. G. Falkowski, and D. H. Turpin. 1989. Respiratory losses in the light in a marine diatom: measurements by short-term mass spectrometry. Limnol. Oceanogr. 34: 1153-1161.

Welschmeyer, N. A., and C. Lorenzen. 1981. Chlorophyll-specific photosynthesis and quantum efficiency at subsaturating light intensities. J. Phycol. 17: 283-293.

Williams, P. J. leB. 1993. Chemical and tracer methods of measuring plankton production. ICES Mar. Sci. Symp. 197: 20-36.

Williams, P. J. leB., R. C. T. Raine, and J. R. Bryan. 1979. Agreement between the ^{14}C and oxygen methods of measuring phytoplankton production: reassessment of the photosynthetic quotient. Oceanol. Acta 2: 411-416.

Williams, P. J. leB., and J. I. Robertson. 1989. A serious inhibition problem from a Niskin sampler during plankton productivity studies. Limnol. Oceanogr. 34: 1300-1305.

Williams, P. J. leB., and J. E. Robertson. 1991. Overall planktonic oxygen and carbon dioxide metabolisms: The problem of reconciling observations and calculations of photosynthetic quotients. J. Plank. Res. 13 (Suppl.): 153-169.

Woodwell, G. M., R. H. Whittaker, W. A. Reiners, G. E. Likens, C. C. Delwiche, and D. B. Botkin. 1978. The biota and the world carbon budget. Science 199: 141-146.

Yamamoto, H. Y., and C. O. Chichester. 1965. Dark incorporation of $^{18}O_2$ into antheroxanthin by bean leaf. Biochem. Biophys. Acta 109: 303-305.

Yoder, J. A., S. G. Ackleson, R. T. Barber, P. Flament, and W. M. Balch. 1994. A line in the sea. Nature 371: 689-692.

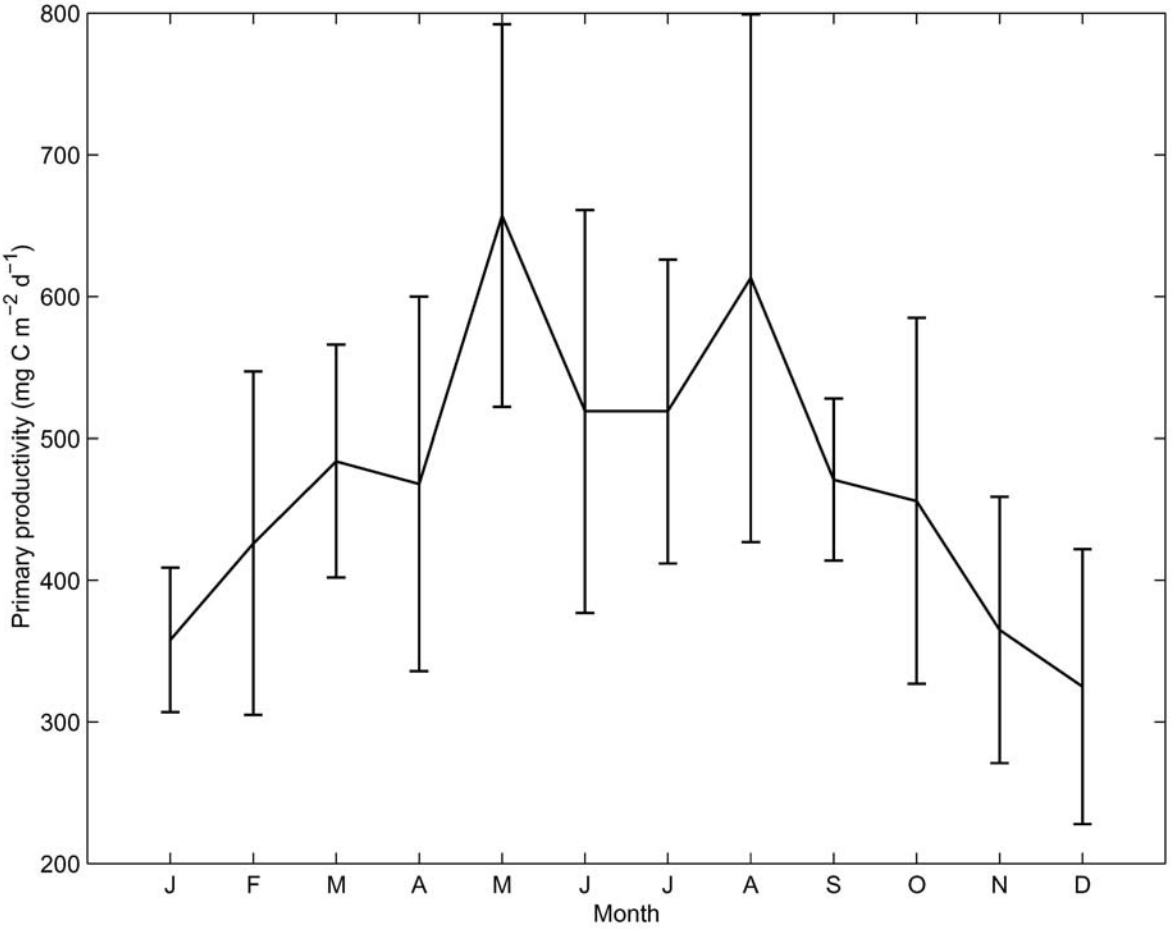

Figure 1. The pattern of primary productivity at station ALOHA (22° 45'N, 158°W) over the course of a year based on data collected from 1989 through 1999. (http://hahana.soest.hawaii.edu/hot/hot-dogs/ppseries.html). Error bars are standard deviations.

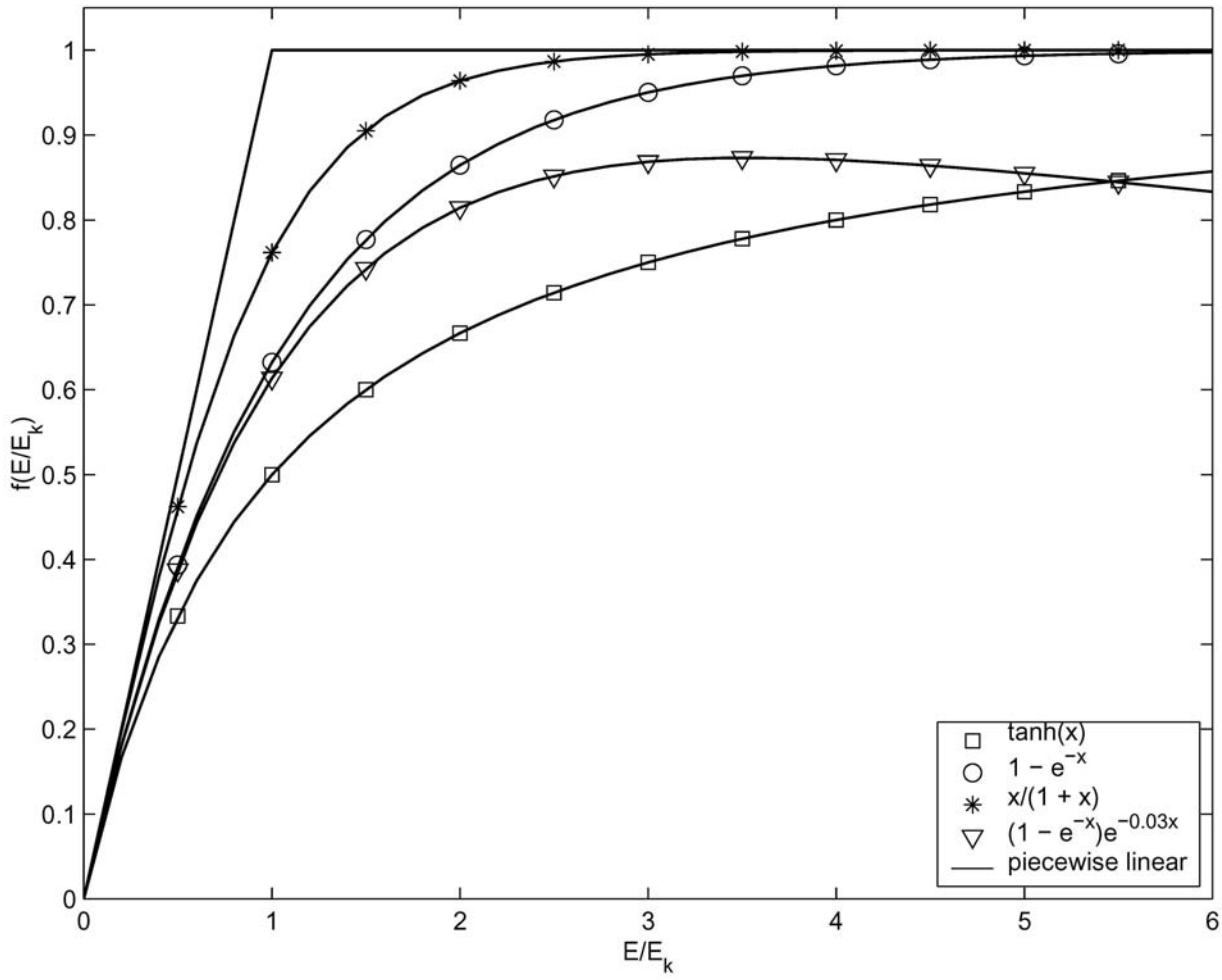

Figure 2. Relationship between E_o/E_k and $f(E_o/E_k)$ for five model equations relating E_o/E_k to photosynthetic rate.

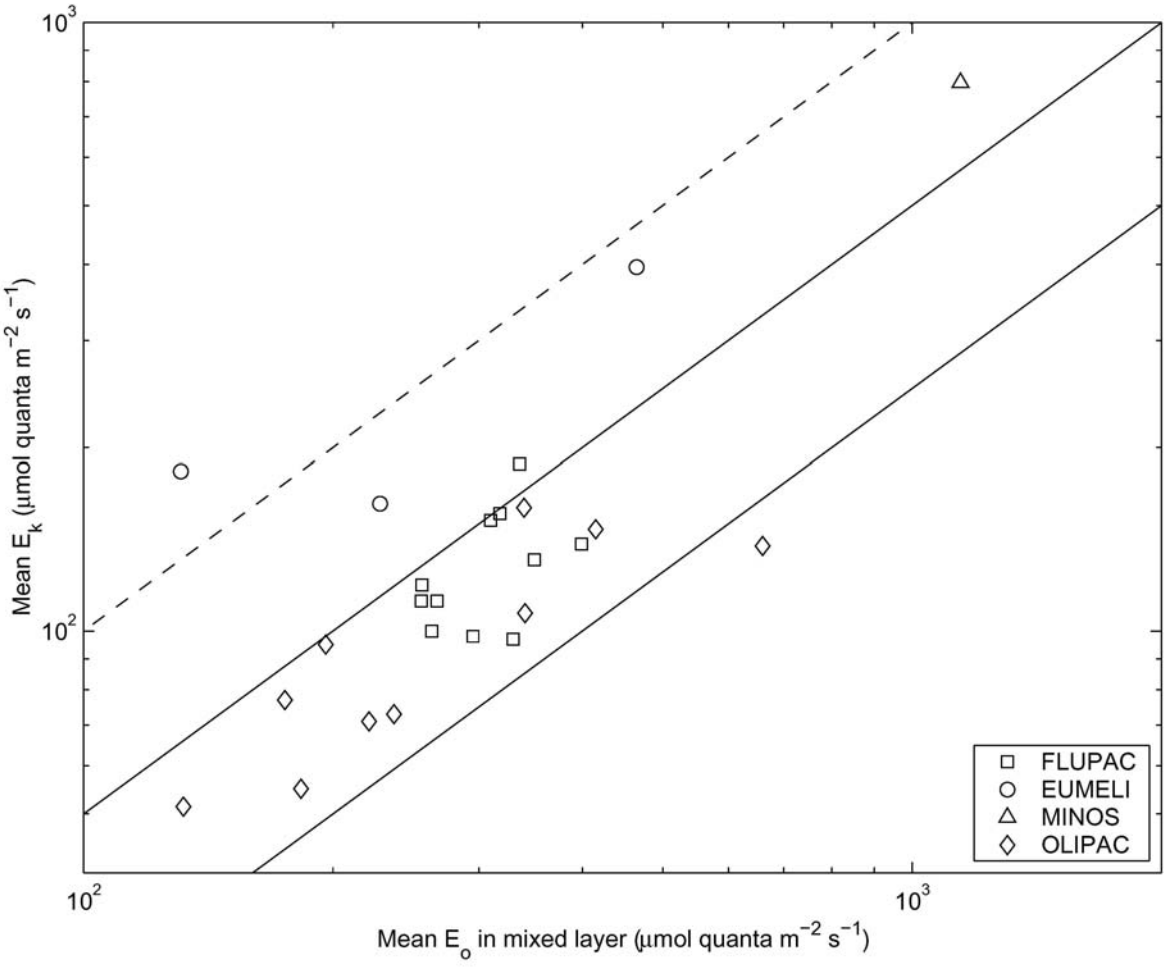

Figure 3. Relationship between the mean E_o in the mixed layer and the mean E_k for phytoplankton communities. The dashed line corresponds to $E_o = E_k$. The solid lines correspond to $E_o = 2E_k$ and $E_o = 4E_k$.

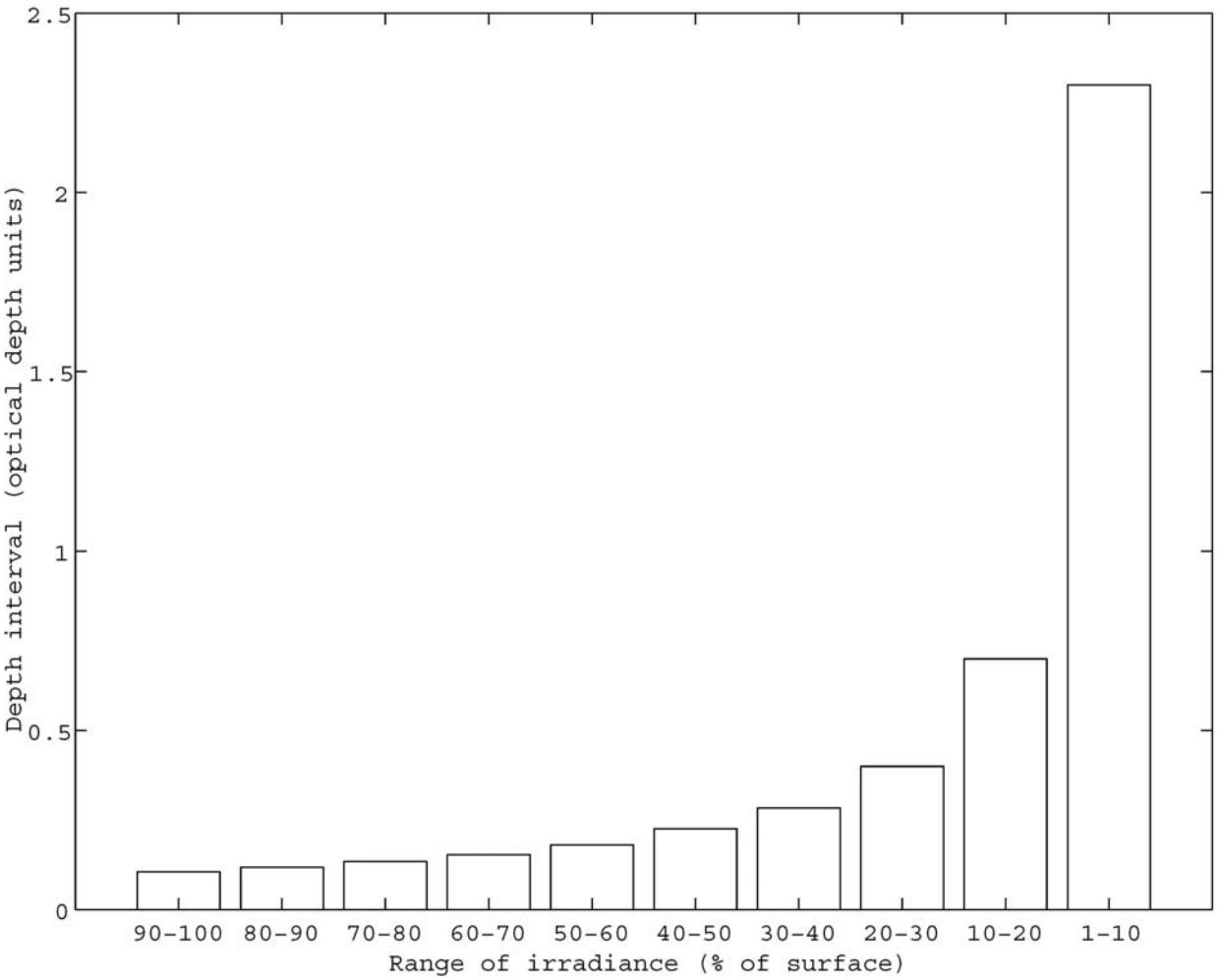

Figure 4. Relationship between range of irradiance and depth interval in a water column in which irradiance decays exponentially with depth.

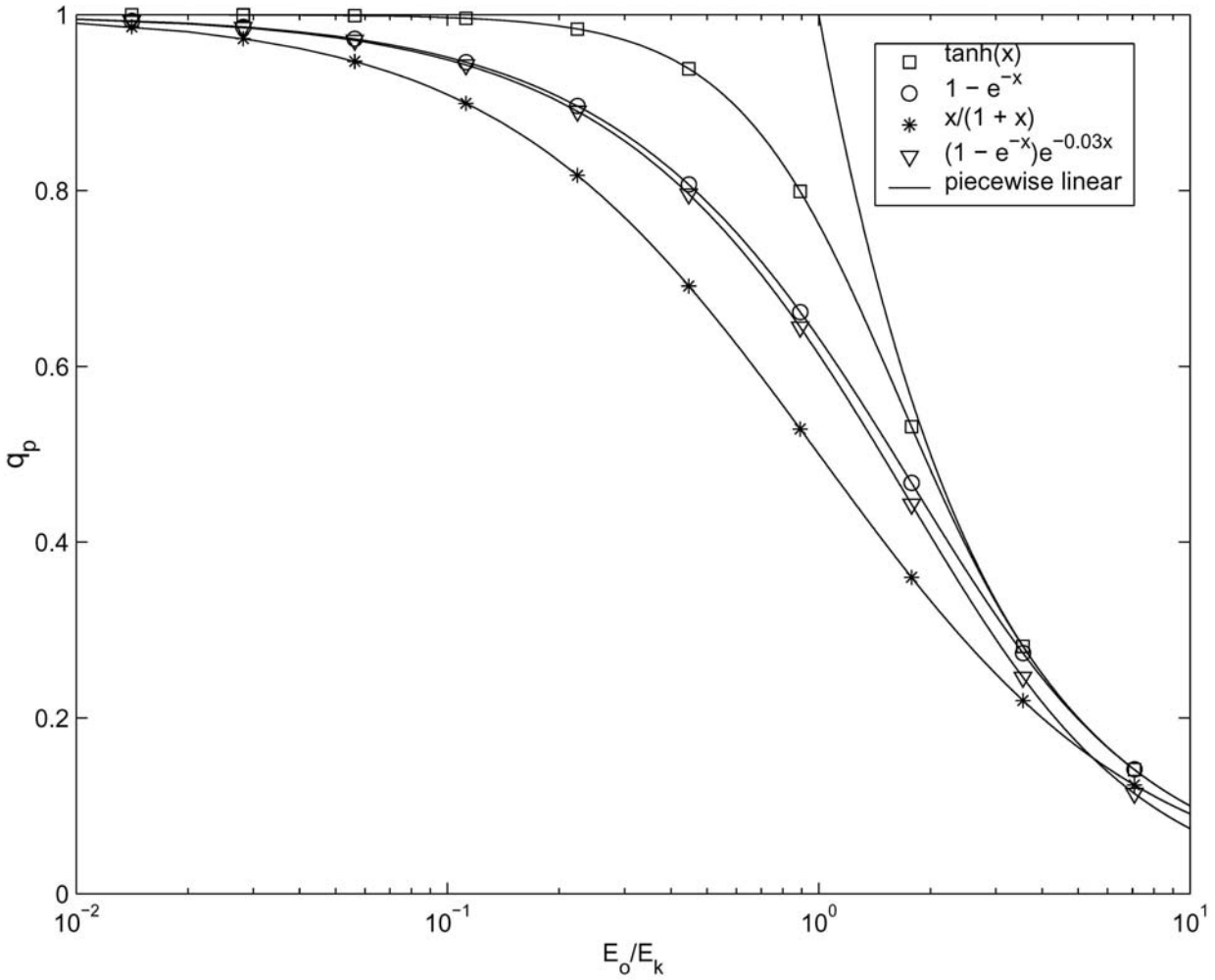

Figure 5. Expected relationship between q_p and E_o/E_k for model equations 4-8.

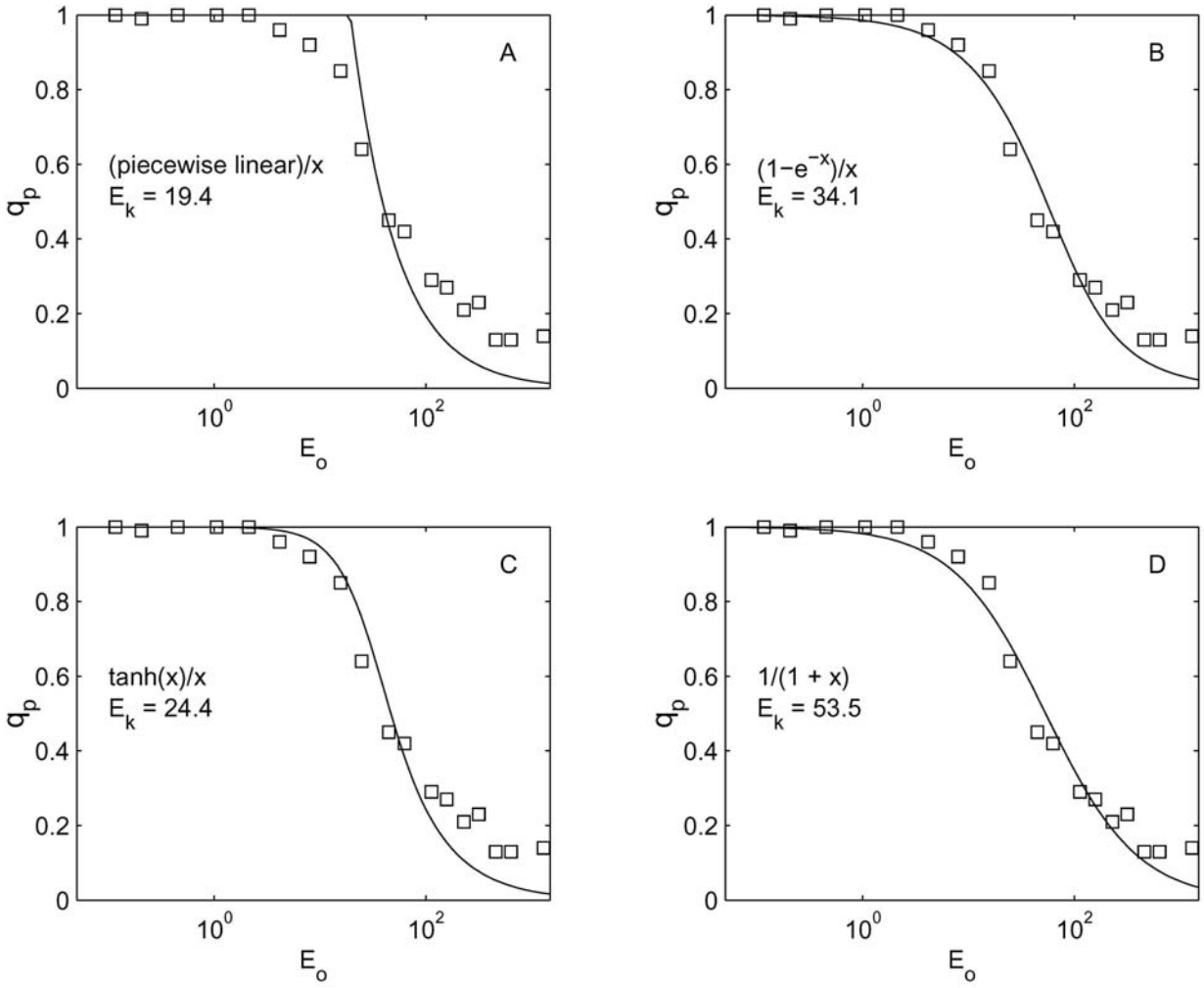

Figure 6. q_p versus irradiance data for *Chaetoceros* sp. grown at 23°C. Of the models tested, the negative exponential (6B) and rectangular hyperbola (6D) formulations for $f(E_o/E_k)$ give the best fit to the data. Although the goodness of fit is virtually identical in these two cases, the calculated E_k values differ by a factor of 1.6.

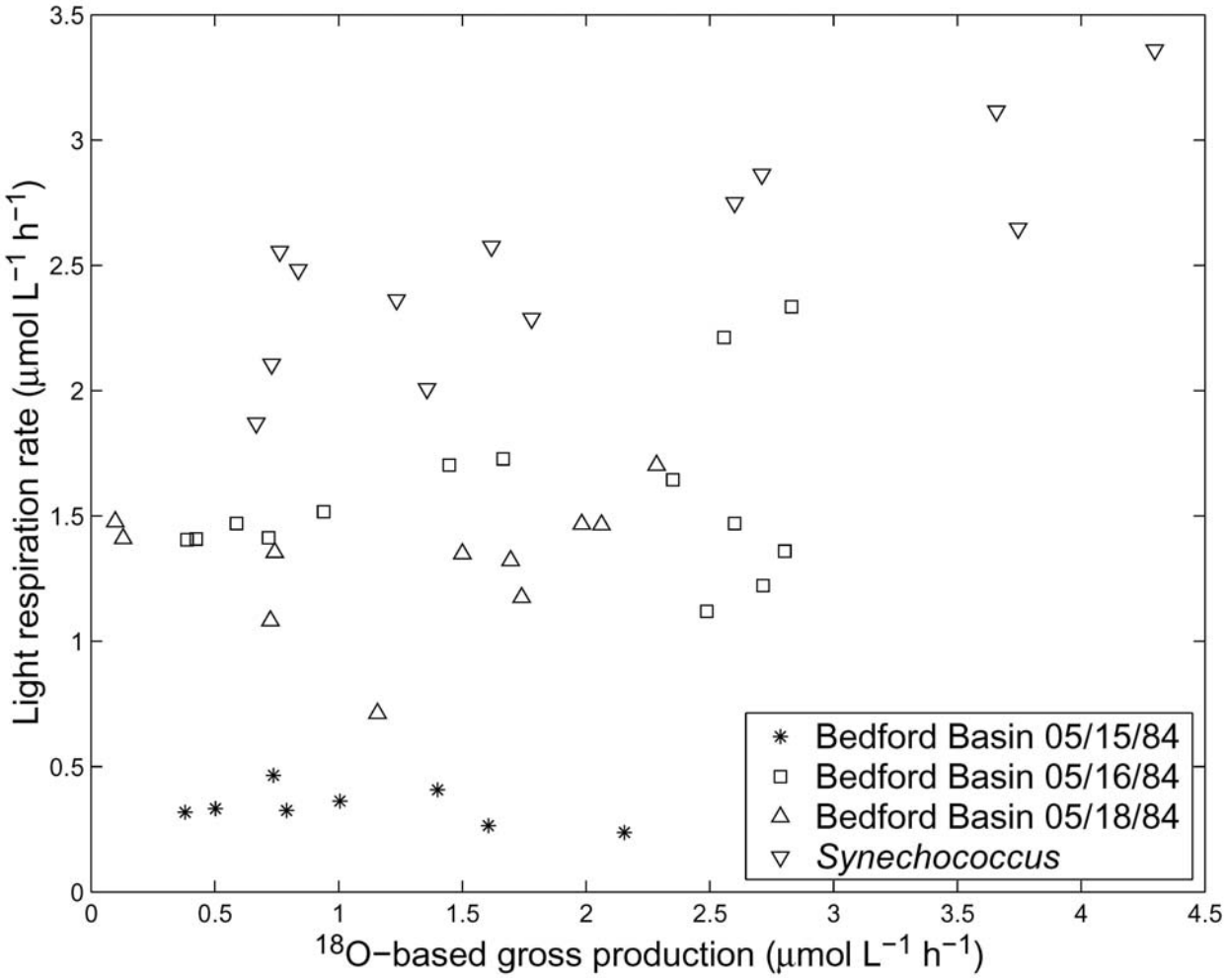

Figure 7. Relationship between Light respiration versus ^{18}O-based gross production and light respiration in four experiments reported by Grande et al. (1991).

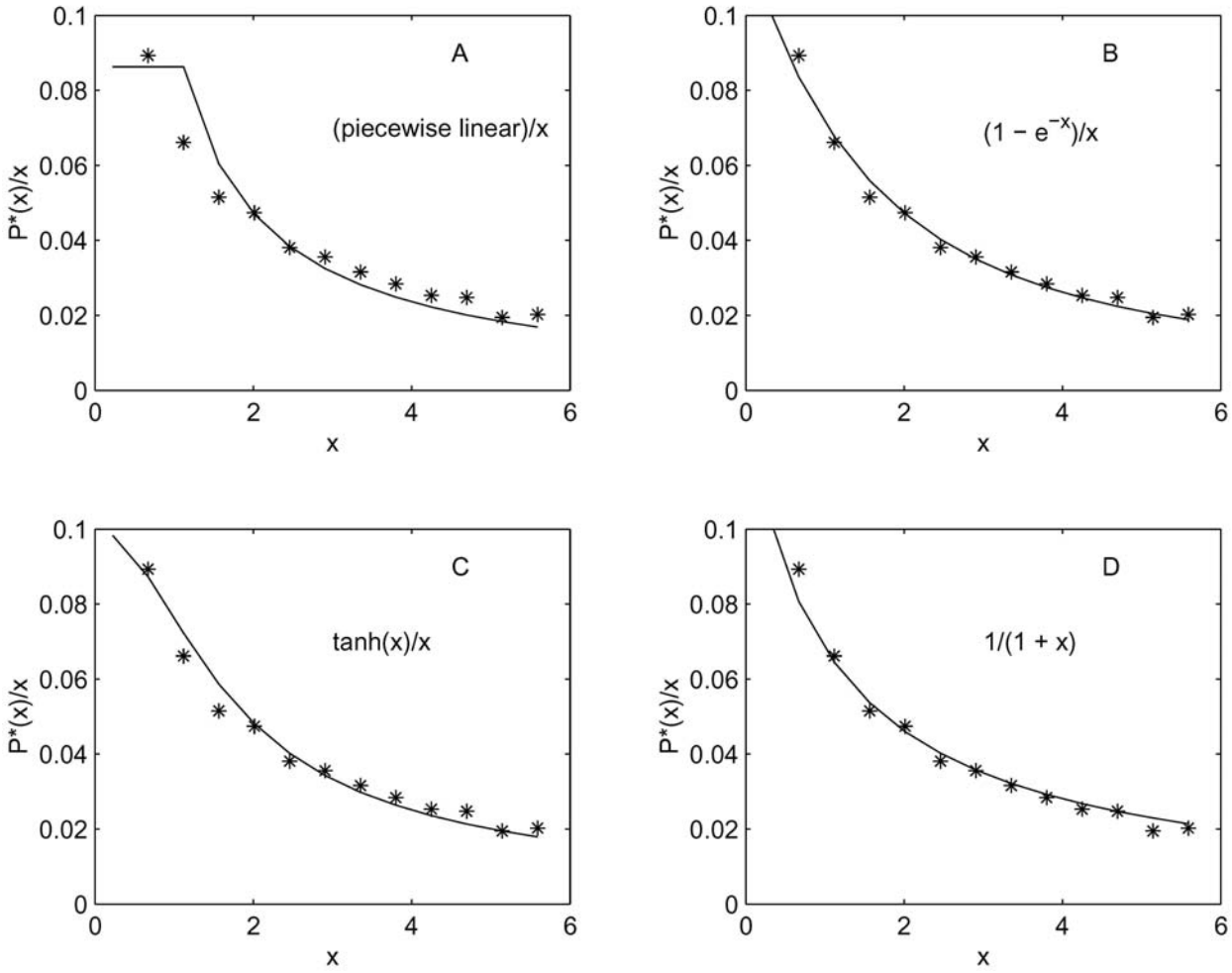

Figure 8. Examples of least squares fits of various functions to noise-corrupted P*(x)/x data which $P^*(x) = 1 - e^{-x}$. The data were noise-corrupted using normally distributed random numbers with a standard deviation equal to 5% of P_m^*.

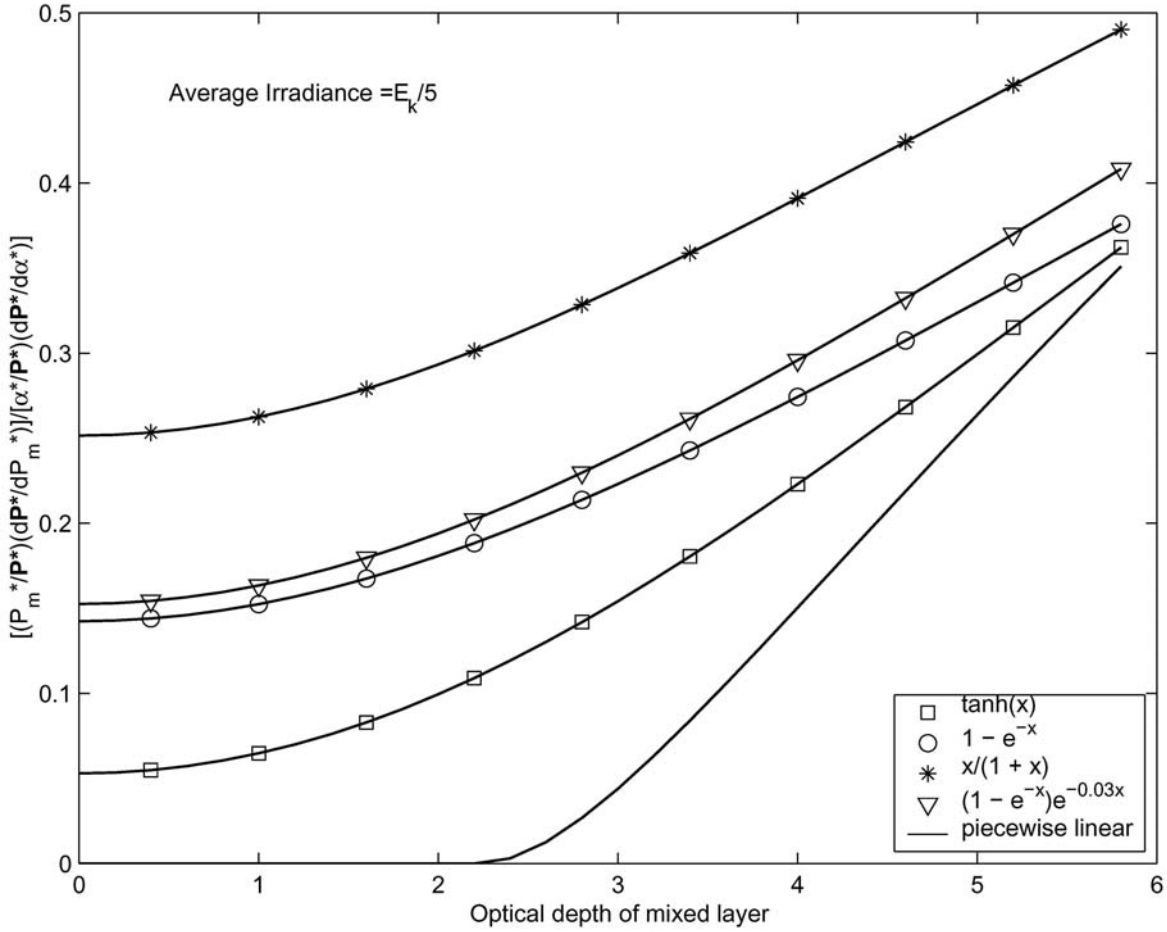

Figure 9. Relationship between optical depth of the mixed layer and $[(P_m^*/\mathbf{P}^*)(\partial\mathbf{P}^*/\partial P_m^*)]/[(\alpha*/\mathbf{P}^*)(\partial\mathbf{P}^*/\partial\alpha*)]$ when the average irradiance in the mixed layer equals $E_k/5$. Symbols as in Fig 2.

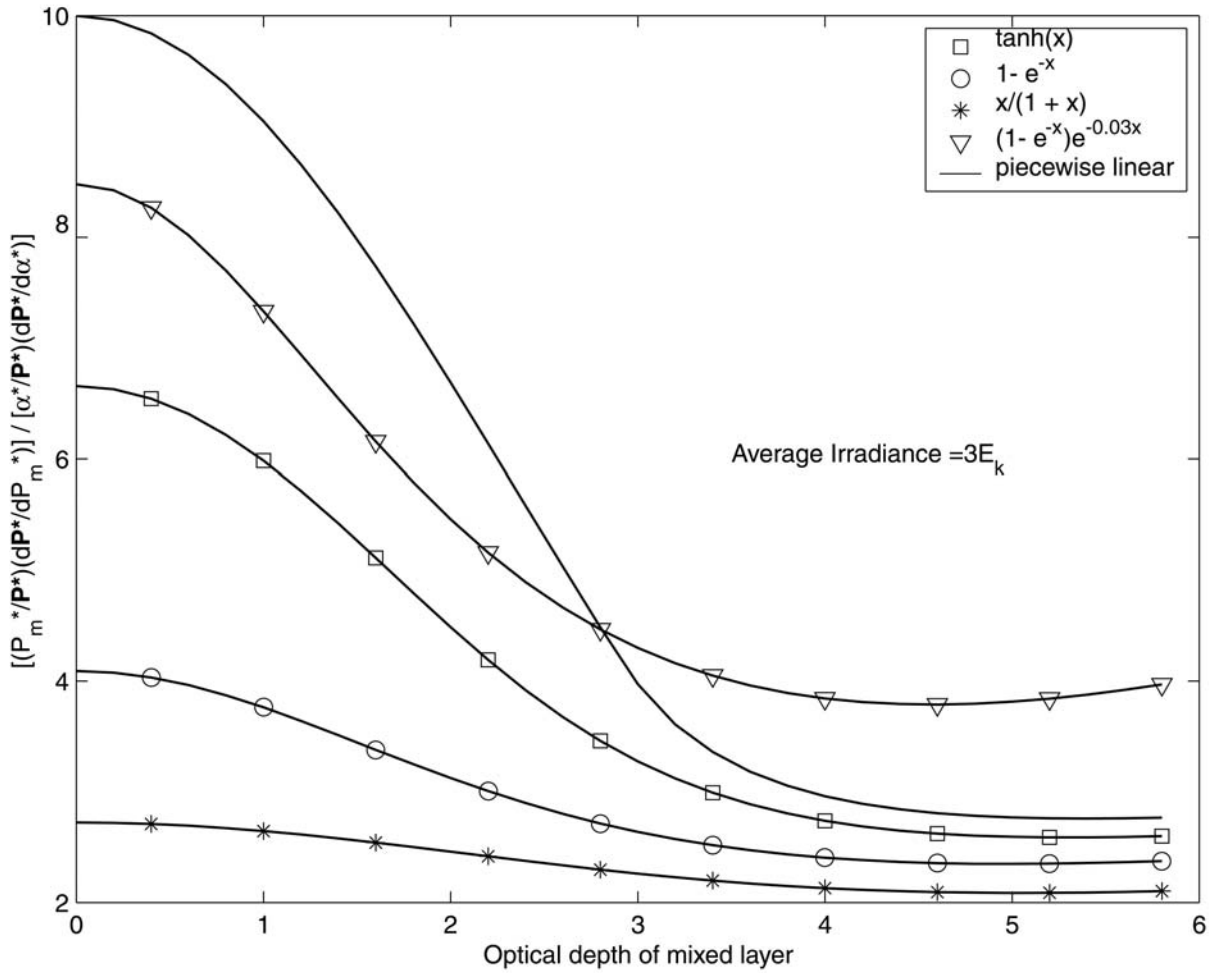

Figure 10. Relationship between optical depth of the mixed layer and

$[(\mathrm{P}_{\mathrm{m}}^{*}/\mathbf{P}^{*})(\partial\mathbf{P}^{*}/\partial\,\mathrm{P}_{\mathrm{m}}^{*})]/[(\alpha*/\mathbf{P}^{*})(\partial\mathbf{P}^{*}/\partial\alpha*)]$ when the average irradiance in the mixed layer equals $3E_k$. Symbols as in Fig. 2.

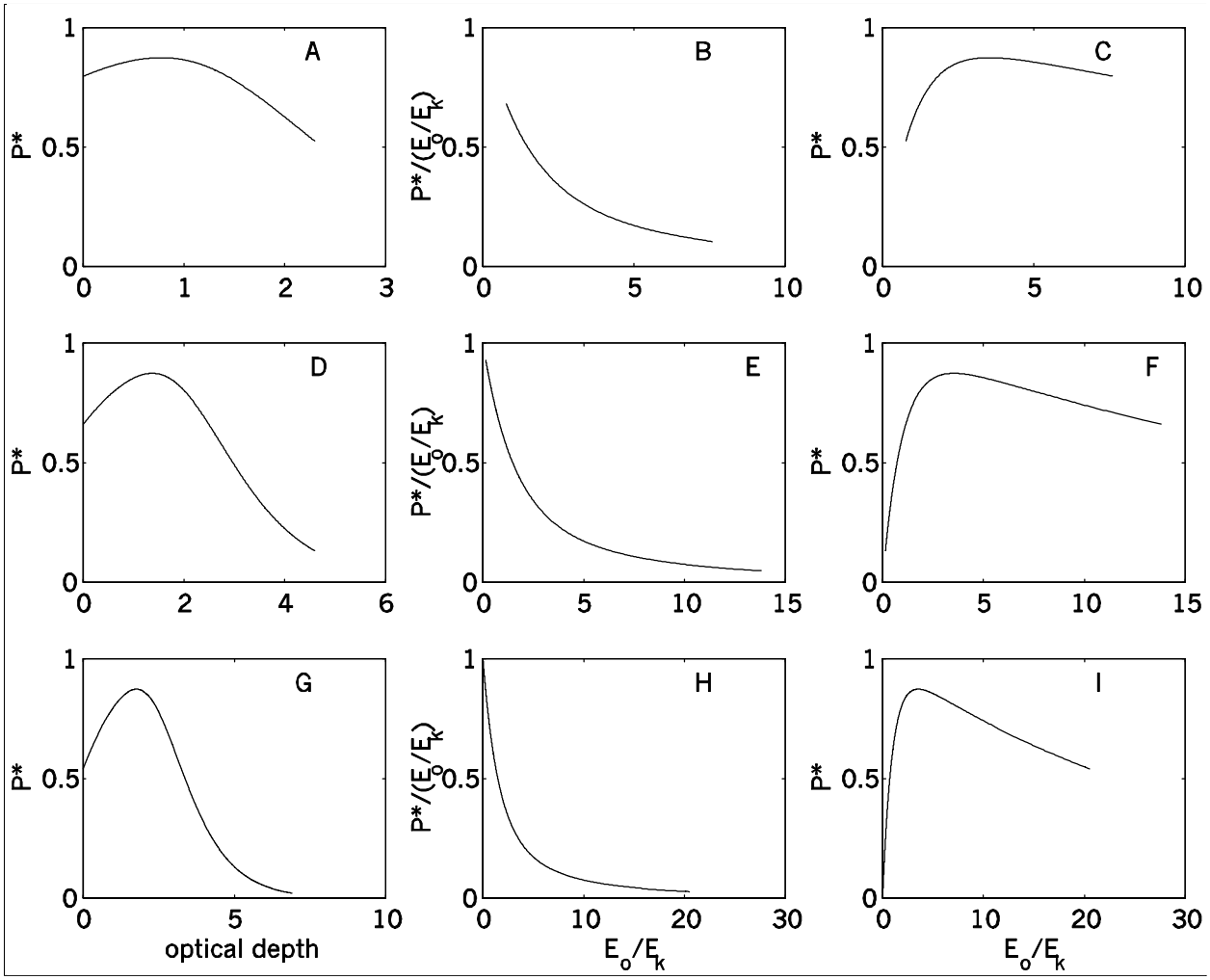

Figure 11. Comparative plots of P* vs. optical depth, $P^*/(E_o/E_k)$ vs. E_o/E_k, and P* vs. E_o/E_k for mixed layers with optical depths of 2.3, 4.6, and 6.9. In each case E_k was assumed to equal 1/3 of the average irradiance in the mixed layer.

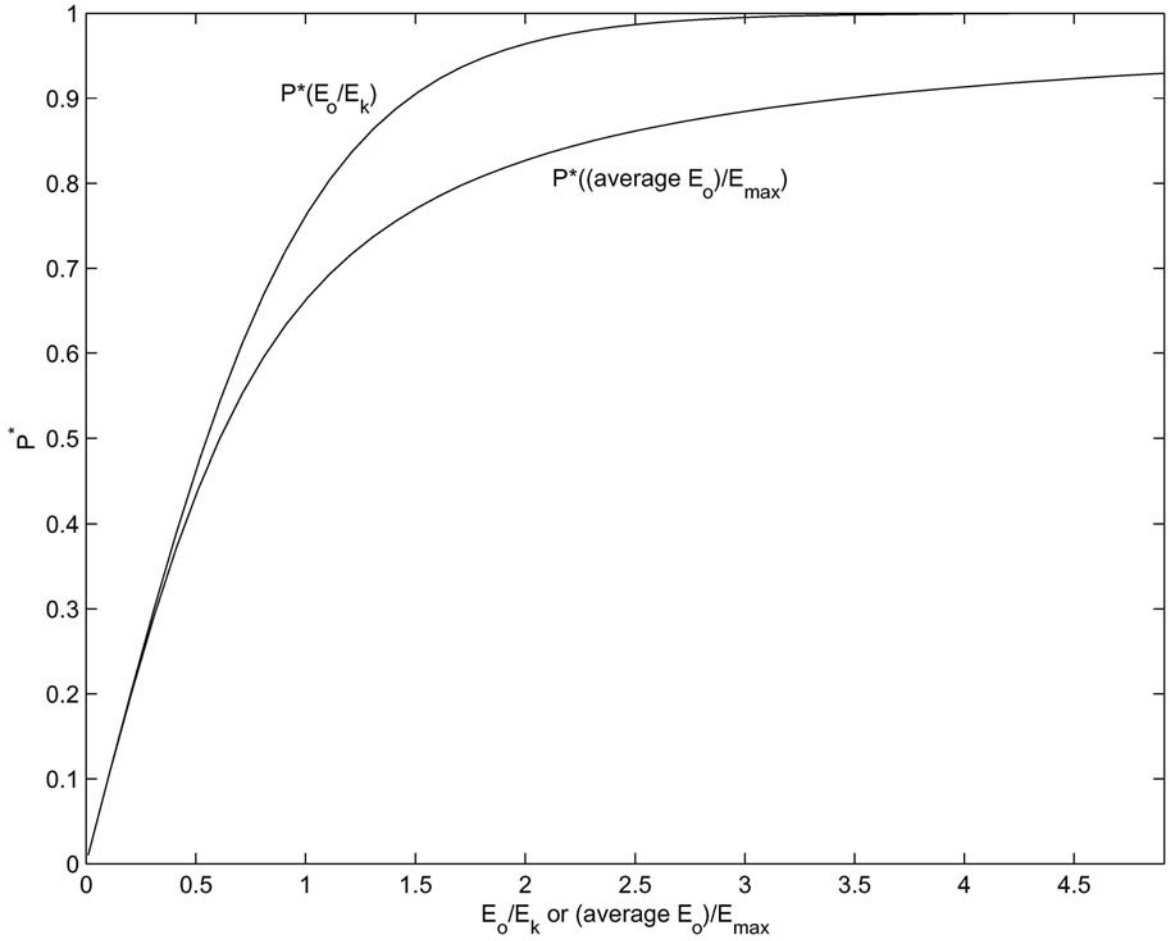

Figure 12. Relationship between P* and E_o/E_k or $\overline{E}_o/E_{max}$ for the simple case where $P^*(E_o/E_k) = \tanh(E_o/E_k)$ and E_o is a linear function of time from sunrise to midday.

The JGOFS Report Series includes the following:

1 Report of the Second Session of the SCOR Committee for JGOFS. The Hague, September 1988
2 Report of the Third Session of the SCOR Committee for JGOFS. Honolulu, September 1989
3 Report of the JGOFS Pacific Planning Workshop. Honolulu, September 1989
4 JGOFS North Atlantic Bloom Experiment: Report of the First Data Workshop. Kiel, March 1990
5 Science Plan. August 1990
6 JGOFS Core Measurement Protocols: Reports of the Core Measurement Working Groups
7 JGOFS North Atlantic Bloom Experiment, International Scientific Symposium Abstracts. Washington, November 1990
8 Report of the International Workshop on Equatorial Pacific Process Studies. Tokyo, April 1990
9 JGOFS Implementation Plan. (also published as IGBP Report No. 23) September 1992
10 The JGOFS Southern Ocean Study
11 The Reports of JGOFS meetings held in Taipei, October 1992: Seventh Meeting of the JGOFS Scientific Steering Committee; Global Synthesis in JGOFS - A Round Table Discussion; JGOFS Scientific and Organizational Issues in the Asian Region - Report of a Workshop; JGOFS/LOICZ Continental Margins Task Team - Report of the First Meeting. March 1993
12 Report of the Second Meeting of the JGOFS North Atlantic Planning Group
13 The Reports of JGOFS meetings held in Carqueiranne, France, September 1993: Eighth Meeting of the JGOFS Scientific Steering Committee; JGOFS Southern Ocean Planning Group - Report for 1992/93; Measurement of the Parameters of Photosynthesis - A Report from the JGOFS Photosynthesis Measurement Task Team. March 1994
14 Biogeochemical Ocean-Atmosphere Transfers. A paper for JGOFS and IGAC by Ronald Prinn, Peter Liss and Patrick Buat-Ménard. March 1994
15 Report of the JGOFS/LOICZ Task Team on Continental Margin Studies. April 1994
16 Report of the Ninth Meeting of the JGOFS Scientific Steering Committee, Victoria, B.C. Canada, October 1994 and The Report of the JGOFS Southern Ocean Planning Group for 1993/94
17 JGOFS Arabian Sea Process Study. March 1995
18 Joint Global Ocean Flux Study: Publications, 1988-1995. April 1995
19 Protocols for the Joint Global Ocean Flux studies (JGOFS) core measurements (reprint). June 1996
20 Remote Sensing in the JGOFS programme. September 1996
21 First report of the JGOFS/LOICZ Continental Margins Task Team. October 1996
22 Report on the International Workshop on Continental Shelf Fluxes of Carbon, Nitrogen and Phosphorus. 1996
23 One-Dimensional models of water column biogeochemistry. Report of a workshop held in Toulouse, France, November-December 1995. February 1997
24 Joint Global Ocean Flux Study: Publications, 1988-1996. October 1997
25 JGOFS/LOICZ Workshop on Non-Conservative Fluxes in the Continental Margins. October 1997
26 Report of the JGOFS/LOICZ Continental Margins Task Team Meeting, No 2. October 1997
27 Parameters of photosynthesis: definitions, theory and interpretation of results. August 1998
28 Eleventh meeting of the JGOFS SSC; Twelfth meeting of the JGOFS SSC; and the Second meeting of the North Pacific Task Team. November 1998
29 JGOFS Data Management and Synthesis Workshop, 25-27 Sept. 1998, Bergen, Norway. Meeting Minutes. January 1999
30 Publications 1988-1999. January 2000
31 Thirteenth meeting of the JGOFS Scientific Steering Committee. Fourteenth meeting of the JGOFS Scientific Steering Committee. Fifteenth meeting of the JGOFS Scientific Steering Committee. October 2001
32 Meeting of the Southern Ocean Synthesis Group, Year 1998. October 2001
33 Joint IGBP EU-US Meeting on the Ocean Component of an integrated Carbon Cycle Science Framework. October 2001
34 First Meeting of the North Atlantic Synthesis Group, 1998; Second Meeting of the North Atlantic Synthesis Group, 1999; Third Meeting of the North Atlantic Synthesis Group, 2001. October 2001
35 Report of the Indian Ocean Synthesis Group on the Arabian Sea Process Study. January 2002

The following reports were published by SCOR in 1987 - 1989 prior to the establishment of the JGOFS Report Series:

- The Joint Global Ocean Flux Study: Background, Goals, Organizations, and Next Steps. Report of the International Scientific Planning and Coordination Meeting for Global Ocean Flux Studies. Sponsored by SCOR. Held at ICSU Headquarters, Paris, 17-19 February 1987
- North Atlantic Planning Workshop. Paris, 7-11 September 1987
- SCOR Committee for the Joint Global Ocean Flux Study. Report of the First Session. Miami, January 1988
- Report of the First Meeting of the JGOFS Pilot Study Cruise Coordinating Committee. Plymouth, UK, April 1988
- Report of the JGOFS Working Group on Data Management. Bedford Institute of Oceanography, September 1988